2018

Calibrating amino acid $\delta^{13}C$ and $\delta^{15}N$ offsets between polyp and protein skeleton to develop proteinaceous deep-sea corals as paleoceanographic archives.

Kelton W. McMahon
University of Rhode Island, kelton_mcmahon@uri.edu

Branwen Williams

Citation/Publisher Attribution

McMahon, K. W., Williams, B., Guilderson, T. P., Glynn, D. S., & McCarthy, M. D. (2018). Calibrating amino acid $\delta^{13}C$ and $\delta^{15}N$ offsets between polyp and protein skeleton to develop proteinaceous deep-sea corals as paleoceanographic archives. *Geochemica et Cosmochimica Acta, 220*, 261-275. doi: 10.1016/j.gca.2017.09.048.
Available at: https://doi.org/10.1016/j.gca.2017.09.048

Calibrating amino acid $\delta^{13}C$ and $\delta^{15}N$ offsets between polyp and protein skeleton to develop proteinaceous deep-sea corals as paleoceanographic archives.

Kelton W. McMahon[a,b,c*], Branwen Williams[c], Thomas P. Guilderson[b,e], Danielle S. Glynn[d], and Matthew D. McCarthy[d]

[a]Graduate School of Oceanography, University of Rhode Island, Narragansett, RI 02882 USA

[b]Institute of Marine Sciences, University of California – Santa Cruz, Santa Cruz, CA 95064 USA

[c]W.M. Keck Science Department of Claremont McKenna College, Pitzer College, and Scripps College, Claremont, CA 91711, USA

[d]Ocean Sciences Department, University of California – Santa Cruz, Santa Cruz, CA 95064 USA

[e]Lawrence Livermore National Laboratory, Livermore, California 94550, USA.

*Corresponding Author: K. McMahon (kelton_mcmahon@uri.edu)

Co-authors: B. Williams (bwilliams@kecksci.claremont.edu); T. Guilderson (guilderson1@llnl.gov); D. Glynn (dglynn@ucsc.edu); M. McCarthy (mdmccar@ucsc.edu)

Abbreviations as a footnote

AA: Amino acid; CSI-AA: Compound-specific stable isotopes of amino acids; SIA: Stable isotope analysis; SIAR: Stable Isotope Analysis in R; TP_{CSI-AA}: Trophic position from compound-specific stable isotopes of amino acids.

ABSTRACT

Compound-specific stable isotopes of amino acids (CSI-AA) from proteinaceous deep-sea coral skeletons has the potential to improve paleoreconstructions of plankton community composition, and our understanding of the trophic dynamics and biogeochemical cycling of sinking organic matter in the Ocean. However, the assumption that the molecular isotopic values preserved in protein skeletal material reflect those of the living coral polyps has never been directly investigated in proteinaceous deep-sea corals. We examined CSI-AA from three genera of proteinaceous deep-sea corals from three oceanographically distinct regions of the North Pacific: *Primnoa* from the Gulf of Alaska, *Isidella* from the Central California Margin, and *Kulamanamana* from the North Pacific Subtropical Gyre. We found minimal offsets in the $\delta^{13}C$ values of both essential and non-essential AAs, and in the $\delta^{15}N$ values of source AAs, between paired samples of polyp tissue and protein skeleton. Using an essential AA $\delta^{13}C$ fingerprinting approach, we show that estimates of the relative contribution of eukaryotic microalgae and prokaryotic cyanobacteria to the sinking organic matter supporting deep-sea corals are the same when calculated from polyp tissue or recently deposited skeletal tissue. The $\delta^{15}N$ values of trophic AAs in skeletal tissue, on the other hand, were consistently 3-4‰ lower than polyp tissue for all three genera. We hypothesize that this offset reflects a partitioning of nitrogen flux through isotopic branch points in the synthesis of polyp (fast turnover tissue) and skeleton (slow, unidirectional incorporation). This offset indicates an underestimation, albeit correctable, of approximately half a trophic position from gorgonin protein-based deep-sea coral skeleton. Together, our observations open the door for applying many of the rapidly evolving CSI-AA based tools developed for metabolically active tissues in modern systems to archival coral tissues in a paleoceanographic context.

1. INTRODUCTION

A diverse array of analytical tools is used to examine ocean ecosystem and biogeochemistry cycling responses to changing climatic conditions (Gordon and Morel 1983; Henderson 2002; Rothwell and Rack 2006; Katz et al. 2010). However, there is a critical gap in resolution between short-term, high-resolution instrumental records, such as remote satellite sensing, and most long-term, paleoceanographic sediment records. The geochemical composition of well preserved, accretionary biogenic tissues (hereafter bioarchives) has the potential to close this gap, shedding light on the structure and function of past ocean ecosystems and their responses to changing climatic and oceanographic conditions on the scale of decades to millennia (Druffel 1997; Barker et al. 2005; Ehrlich 2010; Robinson et al. 2014).

Deep-sea (azooxanthellate) corals were discovered over two hundred years ago (Roberts and Hirshfield 2004), yet their potential as bioarchives of past ocean conditions is just starting to be fully appreciated (Robinson et al. 2014). They are found on hard substrates in every ocean from near the surface to over 6000 m water depth (Cairns 2007). They provide a direct link to surface ocean processes by feeding opportunistically on recently exported surface-derived, sinking particulate organic matter (POM) akin to a "living sediment trap" (Ribes et al. 1999; Orejas et al. 2003; Roark et al. 2009). In the case of proteinaceous deep-sea corals, their skeletons are made of an extremely durable, cross-linked, fibrillar protein that is among the most diagenetically resistant proteinaceous materials known (Goldberg 1974; Ehrlich 2010; Strzepek et al. 2014). Proteinaceous skeletons are deposited in growth layers that are not metabolically reworked post-deposition (Roark et al. 2009; Sherwood and Edinger 2009), and many species can live for hundreds to thousands of years (Roark et al. 2006, 2009; Guilderson et al. 2013). As such, proteinaceous deep-sea corals can be long-term (millennial), high-resolution (annual to

70 decadal) bioarchives of past ocean conditions.

71 Much of the recent proxy development work with proteinaceous deep-sea corals has
72 focused on stable isotope analysis (SIA) of total ("bulk") skeletal material, as a proxy for
73 changes in surface ocean conditions (e.g., Heikoop et al. 2002; Sherwood et al. 2005, 2009;
74 Williams et al. 2007; Hill et al. 2014). A main challenge to interpreting bulk stable isotope data
75 in a paleo-context is determining whether changes in bulk stable isotope values are due to 1)
76 changes in baseline dissolved inorganic carbon (^{13}DIC) or $^{15}NO_3$ values, 2) changes in plankton
77 community composition, 3) changes in trophic dynamics of organic matter exported from the
78 surface ocean (export production) or corals themselves, 4) changes in microbial reworking of
79 sinking organic matter, or some combination of all of these factors (Wakeham and Lee 1989;
80 Meyers 1994; Lehmann et al. 2002; Post 2002). Compound-specific stable isotopes of individual
81 amino acids (CSI-AA) offer a powerful suite of new tools to begin teasing apart these
82 confounding variables (reviewed in Ohkouchi et al. 2017).

83 The potential of CSI-AA in paleoceanographic studies lies in the differential fractionation
84 of individual AAs between diet and consumer. With respect to $\delta^{13}C$, there is a high degree of
85 metabolic diversity in essential AA synthesis pathways among distinct lineages of primary
86 producers (Hayes 2001; Scott et al. 2006), which leads to unique essential AA $\delta^{13}C$
87 "fingerprints" of primary producers (Larsen et al. 2009, 2013; McMahon et al. 2011, 2015a,
88 2016). While the phylogenetic specificity of this approach is still coarse and will inherently be
89 limited by the underlying diversity in central metabolism pathways among primary producers,
90 our ability to identify primary producers at finer taxonomic scales using CSI-AA is improving
91 (e.g., Larsen et al. 2009, 2013; McMahon et al. 2015a). These isotopic fingerprints are passed on
92 to upper trophic level consumers, virtually unmodified, because animals acquire essential AAs

93 directly from their diet (Reeds 2000) with little to no isotopic fractionation between diet and
94 consumer (Hare et al. 1991; Howland et al. 2003; McMahon et al. 2010). As a result, essential
95 AA $\delta^{13}C$ fingerprinting tools are now rapidly developing, with the ultimate goal of quantifying
96 the primary producer sources in food webs (e.g., Arthur et al. 2014; Nielsen and Winder 2015;
97 McMahon et al. 2016).

98 With respect to $\delta^{15}N$, individual AAs are commonly divided into trophic and source AAs
99 (after Popp et al. 2007) based on their relative ^{15}N fractionation with trophic transfer ($\Delta^{15}N_{C\text{-}D}$)
100 (reviewed in McMahon and McCarthy 2016; Ohkouchi et al. 2017). Source AAs (e.g.,
101 phenylalanine: Phe) exhibit minimal nitrogen isotope fractionation during trophic transfer
102 (McClelland and Montoya 2002; Chikaraishi et al. 2009; McMahon et al. 2015b). Thus $\delta^{15}N_{Phe}$
103 has commonly been used as a proxy for the sources and cycling of nitrogen at the base of food
104 webs ($\delta^{15}N_{baseline}$) (Décima et al. 2013; Sherwood et al. 2014; Vokhshoori and McCarthy 2014;
105 Lorrain et al. 2015). Trophic AAs (e.g., glutamic acid: Glu), on the other hand, undergo
106 significant nitrogen isotope fractionation during transamination/deamination (McClelland and
107 Montoya 2002; Chikaraishi et al. 2009). When utilized together, the CSI-AA approach provides
108 a metric of trophic position that is internally indexed to the $\delta^{15}N_{baseline}$ (Chikaraishi et al. 2007;
109 Chikaraishi et al. 2009). It is important to note that the processes for AA $\delta^{15}N$ fractionation
110 (degree of transamination/deamination; Braun et al. 2014) are largely independent from the
111 processes for AA $\delta^{13}C$ fractionation (ability to synthesize carbon side chains; Hayes 2001),
112 providing complementary but distinct insight into the processing of organic matter.

113 In recent years, CSI-AA has increasingly been applied to proteinaceous deep-sea corals,
114 with both AA $\delta^{13}C$ and $\delta^{15}N$ analyses used to understand shifting current systems on the Atlantic
115 margin (Sherwood et al. 2011), changes in plankton community composition and nitrogen-

116 fixation in the central Pacific (Sherwood et al., 2014; McMahon et al., 2015a), effects of long-
117 term land use change on Gulf of Mexico N cycling (Prouty et al., 2014), and stability of
118 mesophotic primary productivity in the western Pacific warm pool (Williams et al. 2016).
119 However, a fundamental assumption for all such CSI-AA applications is that individual AA
120 stable isotope values of bioarchival skeleton material reflect the same AA isotope values in the
121 metabolically active polyp tissue at the time of deposition. While AA stable isotope values have
122 been well studied in metabolically active consumer tissues (reviewed in McMahon and
123 McCarthy 2016), these structural proteins typically have very different AA compositions and
124 turnover rates (Ehrlich 2010), which could potentially lead to differences in fractionation
125 processes (e.g., Schmidt et al. 2004; Chikaraishi et al. 2014; Hebert et al. 2016). To our
126 knowledge, this underlying question of AA $\delta^{13}C$ and $\delta^{15}N$ preservation in structural tissues of
127 deep-sea corals has never been directly evaluated.

128 Here we present the first quantitative examination of individual AA stable isotope values
129 ($\delta^{13}C$ and $\delta^{15}N$) in paired coral polyp tissue and recently deposited protein skeleton for three
130 genera of deep-sea proteinaceous coral from three oceanographically distinct regions of the
131 North Pacific (Fig. 1; Appendix A): Red Tree Coral *Primnoa pacifica* (Family: Primnoidae)
132 from the Gulf of Alaska, Bamboo Coral *Isidella sp*. (Family: Isididae) from the California
133 Current System, and Hawaiian Gold Coral *Kulamanamana haumeaae* (Family: Parazoanthidae)
134 from the North Pacific Subtropical Gyre (NPSG), hereafter referred to as *Primnoa, Isidella,* and
135 *Kulamanamana*, respectively. We tested the hypothesis that there would be no differences in
136 individual AA $\delta^{13}C$ and $\delta^{15}N$ values between polyp tissue and recent skeletal material. We then
137 tested whether metabolically active polyp tissue and proteinaceous skeleton produced the same
138 results for two commonly used CSI-AA proxy approaches. First, we compared plankton

community composition reconstructions from the paired tissue types using an AA $\delta^{13}C$ fingerprinting approach (e.g., McMahon et al. 2015a). Second, we reconstructed the trophic structure and baseline $\delta^{15}N$ values from both tissues, in corals spanning oligotrophic open ocean gyres to coastal eutrophic margins using AA $\delta^{15}N$ values (e.g., Sherwood et al. 2014).

2. METHODS

2.1 Study specimens and locations

2.1.1 Red Tree Coral: *Primnoa*

Primnoa pacifica (Cairns and Bayer 2005) is an octocoral of the family Primnoidae that forms a large fan-shaped gross morphology comprised of a proteinaceous skeleton with radially alternating couplets of calcite and gorgonin material (Risk et al. 2002; Fig. A.1). These corals are slow growing, with radial growth rates of 100-300 μm yr^{-1} and lifespans of several hundred years (Andrews et al. 2002; Williams et al. 2007).

Here, five *Primnoa* specimens were collected from the Gulf of Alaska. Four live *Primnoa* were collected in 25 to 200 m water depth in the Gulf of Alaska in summer 2013, two using the H2000 ROV aboard the FSV Alaska Provider from Scripps University and two via bottom trawl. One dead specimen was collected from an unknown depth via bottom trawl in summer 2010 (Fig. 1; Table A.1). The coastal regions of the Gulf of Alaska are iron-rich, sourced from cross-shelf exchange and vertical mixing (Bruland et al., 2001; Childers et al., 2005; Ladd et al., 2005), which support high primary productivity characterized by diatoms and flagellates (Sambrotto and Lorenzen 1986; Strom 2006). In deeper water (400 m), $\delta^{15}N$ of the nitrate is 4-5‰ (Wu et al. 1997). There is a strong seasonal cycle in nitrogen dynamics in the coastal region reflecting the supply of nutrients to the surface waters via upwelling during the early summer followed by

rapid nutrient drawdown by summer phytoplankton blooms as the summer progresses and upwelling stops (Wu et al. 1997).

2.1.2 Bamboo coral: *Isidella*

Isidella sp. (Gray 1857) is an octocoral of the family Isididae that forms a skeleton of high magnesium calcite internodes several centimeters long interspersed by proteinaceous gorgonin organic nodes (4-25 mm long) (Fig. A.1). These coral grow in candelabra-like shapes to heights greater than 2 m (Fig. A.1). They are slow growing (radial growth rates of 50-150 μm yr^{-1}), with lifespans reaching several hundred years (Thresher et al., 2004; Roark et al. 2005).

Here, five live specimens of the genus *Isidella* were collected in 1125-1250 m water depth from the California Margin (Sur Ridge) offshore of central California using the Monterey Bay Area Research Institute (MBARI) ROV Doc Ricketts in the summer of 2014 (Fig. 1; Table A.1). The California Margin is one of the most productive zones of the World Ocean, with strong seasonal coastal upwelling from April through early winter (Strub et al. 1987; Garcia-Reyes and Largier 2012) generating a nutrient-rich environment supporting substantial productivity (Bruland et al. 2001). Sur Ridge in the Central California Margin is a high nutrient and low chlorophyll (HNLC) zone (Hutchins and Bruland 1998; Walker and McCarthy 2012). The southward-flowing California Current bathes this region with NO_3^- of oceanic origin, while the northward-flowing California Undercurrent and the weaker nearshore Davidson Current entrain ^{15}N-enriched NO_3^- associated with enhanced denitrification from the high productivity, low oxygen Eastern Tropical North Pacific (Altabet et al. 1999; Voss et al. 2001; Collins et al. 2003).

2.1.3 Hawaiian Gold Coral: *Kulamanamana*

185 *Kulamanamana haumeaae* (Sinniger et al. 2013) is a parasitic zoantharian of the family
186 Parazoanthidae that secretes a scleroprotein skeleton that covers and eventually extends beyond
187 its host coral colony. This coral forms a sea fan shape with heights of several meters (Parrish
188 2015; Fig. A.1). It is a very long-lived, slow growing coral, with lifespans of thousands of years
189 and radial growth rates of 25-100 μm yr^{-1} (Roark et al. 2006, 2009; Guilderson et al. 2013).
190 Here, three live *Kulamanamana* colonies were collected in 350-410 m water depth from
191 the seamounts in the Hawaiian archipelago using the HURL/NOAA Pisces V submersible in the
192 summer of 2004 and 2007 (Fig. 1; Table A.1) (Guilderson et al. 2013). The NPSG is
193 characterized by exceedingly low dissolved nutrients (<10 nmol NO_3^- in the mixed layer) and is
194 dominated by small cell prokaryotic cyanobacterial production (Karl et al. 2001). The nitrogen
195 balance and controls on new production in this system are not strictly limited by available fixed
196 nitrogen (Eppley et al. 1977), and there is significant nitrogen fixation with characteristically low
197 $\delta^{15}N$ values (Karl et al. 2008; Church et al. 2009).
198
199 **2.2 Sample preparation and analysis**
200 2.2.1 Sample Preparation
201 All coral colonies were rinsed with saltwater followed by distilled water and air-dried
202 prior to being transferred to onshore laboratories. Encrusted polyp tissue was then peeled as a
203 single mass from the skeleton of each coral colony with forceps and dried again at 50°C for 24
204 hrs. After drying, the polyp tissue was homogenized, reflecting a colony wide composite sample.
205 Deep-sea coral polyp tissues are very lipid rich (Hamoutene et al. 2008), and therefore polyp
206 tissue samples were lipid extracted three times following the conventional methanol/chloroform
207 protocol of Bligh and Dyer (1959) prior to analysis of CSI-AA to improve chromatography. The

proteinaceous nodes of *Isidella* were separated from the carbonate internodes with a scalpel according to Schiff et al. (2014). Both *Primnoa* and *Kulamanamana* skeletons were sectioned at the base and polished according to Sherwood et al. (2014). The outermost edge of the protein skeleton (~200 μm radial depth, 5-7 mm band parallel to the growth axis) from all three coral genera was sampled with a computerized Merchantek micromill. Skeleton samples were individually acid washed in 1 N HCl in glass vials for four hours, rinsed three times in Milli-Q water, and dried over night at 50°C to remove calcium carbonate prior to analysis of CSI-AA to improve chromatography.

2.2.2 Stable isotope analysis

Bulk $\delta^{13}C$ and $\delta^{15}N$ values and elemental ratios for coral skeleton material as well as coral polyp material before and after lipid extraction (Appendix B; Table B1) were conducted at University of California, Santa Cruz using standard protocols of the Stable Isotope Laboratory (http://emerald.ucsc.edu/~silab/). Isotope values were corrected using an internal laboratory acetanilide standard, and in turn referenced to international IAEA standards. More detailed descriptions of coral tissue bulk analyses and data interpretation are given in Appendix B.

CSI-AA was conducted on polyp tissue and proteinaceous skeleton using 3 mg for $\delta^{13}C$ and 6 mg for $\delta^{15}N$. Samples were acid hydrolyzed in 1 ml of 6 N HCl at 110°C for 20 hrs to isolate the total free AAs and then evaporated to dryness under a gentle stream of ultra-high purity N_2. All samples were redissolved in 0.01N HCl and passed through 0.45 μm Millipore glass-fiber filters followed by rinses with additional 0.01N HCl. Samples were then passed through individual cation exchange columns (Dowex 50WX* 400 ion exchange resin), rinsed with 0.01 N HCl, and eluted into muffled glassware with 2 N ammonia hydroxide. Dried samples

were derivatized by esterification with acidified iso-propanol followed by acylation with trifluoroacetic anhydride (Silfer et al. 1991). Derivatized samples were extracted with P-buffer (KH_2PO_4 + Na_2HPO_4 in Milli-Q water, pH 7) and chloroform three times with centrifugation (600 g) and organic phase extraction between each round (Ueda et al 1989). Samples were evaporated to dryness under a gentle stream of ultra-high purity N_2 prior to neutralization with 2 N HCl at 110°C for 5 min. Dried samples were acylated once again and then brought up in ethyl acetate for CSI-AA analysis.

For AA $\delta^{13}C$ analyses, the derivatized AAs were injected in split mode at 250°C and separated on a DB-5 column (50 m x 0.5 mm inner diameter; 0.25 μm film thickness; Agilent Technologies, Santa Clara, California, USA) in a Thermo Trace Ultra gas chromatograph (GC) at the University of California, Santa Cruz. The separated AA peaks were analyzed on a Finnegan MAT Delta^{Plus} XL isotope ratio mass spectrometer (IRMS) interfaced to the GC through a GC-C III combustion furnace (960°C) and reduction furnace (630°C). For AA $\delta^{15}N$ analyses, the derivatized AAs were injected in splitless mode at 250 °C and separated on a BPX5 column (60 m x 0.32 mm inner diameter, 1.0 μm film thickness; SGE Analytical Science, Austin, Texas, USA) in the same CG-C-IRMS interfaced through a combustion furnace (980°C), reduction furnace (650°C), and a liquid nitrogen trap.

For carbon, we assigned glutamic acid (Glu), aspartic acid (Asp), alanine (Ala), proline (Pro), glycine (Gly), and serine (Ser) as non-essential AAs, and threonine (Thr), leucine (Leu), isoleucine (Ile), valine (Val), and phenylalanine (Phe) as essential AAs (Reeds 2000). For nitrogen, we assigned Glu, Asp, Ala, Leu, Ile, Pro, Val as trophic AAs, and Phe, Methionine (Met), and Lysine (Lys) as source AAs (Popp et al. 2007). Gly, Ser, and Thr were kept as separate groups given the lack of consensus on degree of trophic fractionation between diet and

consumer (reviewed in McMahon and McCarthy 2016). It should be noted that acid hydrolysis converts glutamine (Gln) and aspartamine (Asn) into Glu and Asp, respectively, due to cleavage of the terminal amine group, resulting in the measurement of combined Gln + Glu (referred to hereby as Glu), and Asn +Asp (referred to hereby as Asp).

Standardization of runs was achieved using intermittent pulses of a CO_2 or N_2 reference gas of known isotopic value and internal nor-Leucine standards. All CSI-AA samples were analyzed in triplicate along with AA standards of known isotopic composition (Sigma-Aldrich Co.). The variability reported for $\delta^{13}C$ and $\delta^{15}N$ value of each AA measured (Table C.1-C.4) therefore represents the analytical variation for n = 3 replicate GC-C-IRMS measurements. The long-term reproducibility of stable isotope values in a laboratory algal standard provides an estimate of full protocol reproducibility (replicate hydrolysis, wet chemistry, and analysis): $\delta^{13}C$ = ± 0.7‰ and $\delta^{15}N$ = ± 0.3‰ (calculated as the long-term SD across >100 separate full analyses, averaged across all individual AAs).

2.3 Data analysis

We used principal component analysis to visualize multivariate patterns in the $\delta^{13}C$ values of individual AAs (Ala, Asp, Gly, Glu, Ile, Leu, Phe, Pro, Ser, Thr, Val) in polyp tissue and skeleton of the three deep-sea coral genera (Appendix C, Table C.5). Individual AA stable isotope offsets were calculated as the difference in isotope value ($\delta^{13}C$ or $\delta^{15}N$) between paired polyp and skeleton samples for each individual from the three genera of deep-sea coral. We used separate one-sample t-tests to determine if individual AA $\delta^{13}C$ and $\delta^{15}N$ offsets between polyp and skeleton were significantly different from zero ($\alpha = 0.05$). For all statistical analyses n = 5 individuals for *Primnoa* and *Isidella* and n = 3 individuals for *Kulamamanama*. All data

277 conformed to the assumptions of their respective statistical tests.

278 We used an AA isotope fingerprinting approach to examine the composition of primary
279 producers fueling export production to deep-sea corals in each of the three study regions: Gulf of
280 Alaska (*Primnoa*), Central California Margin (*Isidella*), and NPSG (*Kulamanamana*) (sensu
281 McMahon et al. 2015a; see Appendix C for details). Briefly, we calculated the relative
282 contribution of key plankton end members (eukaryotic microalgae, prokaryotic cyanobacteria,
283 and heterotrophic bacteria) contributing carbon to each coral colony via export production in a
284 fully Bayesian stable isotope mixing framework (Parnell et al. 2010; Ward et al. 2010) within the
285 Stable Isotope Analysis in R (SIAR) package (R Core team 2013). We used published essential
286 AA $\delta^{13}C$ data (Thr, Ile, Val, Phe, and Leu) from eukaryotic microalgae, cyanobacteria, and
287 heterotrophic bacteria (Larsen et al. 2009, 2013; Lehman 2009) as the source data set for the
288 mixing model (Table C.6). We used normalized essential AA $\delta^{13}C$ values of end members and
289 coral tissues (polyp and skeleton) to facilitate comparisons of the AA $\delta^{13}C$ fingerprints across
290 different regions and growing conditions (see Appendix C for justification). To do this, we
291 subtracted the mean of all five essential AA $\delta^{13}C$ values from each individual essential AA $\delta^{13}C$
292 value for each sample (senus Larsen et al. 2015). In SIAR, we ran 500,000 iterations with an
293 initial discard of the first 50,000 iterations as burn-in. We used separate One-Way Analyses of
294 Variance (ANOVA) with Tukey's Honestly Significant Difference (HSD) post-hoc tests (α =
295 0.05) to look for differences in relative contribution of each end member among the three coral
296 genera. We used separate one-sample t-tests to see if the differences in the relative contribution
297 of potential end members calculated from coral polyp tissue vs. skeleton were significantly
298 different from 0 ($\alpha = 0.05$).

299 We examined the differences in mean trophic AA $\delta^{15}N$ offsets (calculated as the mean

δ^{15}N offset between polyp and skeleton averaged across all trophic AAs for each coral) among the three genera of coral using a One-Way ANVOA and Tukey's HSD post-hoc test ($\alpha = 0.05$). We calculated separate $TP_{CSI\text{-}AA}$ values of deep-sea corals based on the AA δ^{15}N values from polyp tissue and skeleton using the single $TDF_{Glu\text{-}Phe}$ approach of Chikaraishi et al. (2009):

$$TP_{CSI-AA-single\ TDF} = 1 + \left[\frac{\delta^{15}N_{Glu} - \delta^{15}N_{Phe} - \beta}{TDF_{Glu-Phe}}\right] \quad (1)$$

where $\delta^{15}N_{Glu}$ and $\delta^{15}N_{Phe}$ represent the stable nitrogen isotope values of coral Glu and Phe, respectively, β represents the difference in δ^{15}N between Glu and Phe of primary producers (3.4‰ for aquatic cyanobacteria and algae [McClelland & Montoya, 2002; Chikaraishi et al. 2010]), and $TDF_{Glu\text{-}Phe}$ is the literature value of 7.6‰ (Chikaraishi et al. 2009). We then used separate one-sample t-tests to see if the differences in $TP_{CSI\text{-}AA}$ offsets calculated from coral polyp tissue vs. skeleton were significantly different from 0 ($\alpha = 0.05$). All statistics were performed in R version 3.0.2 using RStudio interface version 0.98.501 (R Core team 2013).

3. RESULTS

3.1 Bulk elemental and isotopic composition

Detailed analysis of bulk isotopic and elemental composition for coral skeleton and polyp material is given in Appendix B. The δ^{13}C values for coral skeleton material (-15.9 ± 0.9 ‰) was ~3.5‰ more enriched than lipid-intact polyp material (-19.4 ± 1.0 ‰), though both tissues had consistent δ^{13}C values across all three genera examined (Table B.1). The δ^{13}C values of lipid extracted polyp material (-15.5 ± 0.7 ‰) were 4‰ lower than lipid-intact polyps and very similar to corresponding skeleton material (mean offset -0.4 ± 0.5‰) (Table B.1). Lipid

extraction also altered polyp tissue C/N ratios. Lipid-extracted polyp tissues had much lower C/N ratios (3.1 ± 0.3) than lipid-intact polyps (4.8 ± 0.7) and were very similar to coral proteinaceous skeleton (2.9 ± 0.3). Much like $\delta^{13}C$ values, C/N ratios were consistent across all three genera examined. In contrast, the $\delta^{15}N$ values were more variable among the three genera for both skeleton (mean 13.8 ± 1.0 for *Primnoa*; 16.0 ± 0.7for *Isadella*, and 10.3 ± 0.3 for *Kulamanamana*) and lipid-intact polyp tissue (mean 11.2 ± 0.4 for *Primnoa*; 14.8 ± 0.6 for *Isadella*, and 8.3 ± 0.3 for *Kulamanamana*) (Table B.1). On average, coral polyp tissue was 1.9 ± 0.8‰ more enriched than coral skeleton (Table B.1).

3.2 Amino acid carbon isotopes

Individual AA $\delta^{13}C$ values differed significantly among the three coral genera (Fig. 2), with *Primnoa* from the Gulf of Alaska and *Isidella* from the Sur Ridge generally having more positive AA $\delta^{13}C$ values than *Kulamanamana* from the NPSG. Given the substantially larger differences in individual AA $\delta^{13}C$ values among different coral genera compared to among individuals within a genus, all three corals were separated in multivariate space based on principal component analysis of all eleven AA $\delta^{13}C$ values (Fig. 3, Table C.5).

There was little to no variation in individual AA $\delta^{13}C$ values between skeleton and polyp tissue within an individual: mean $\delta^{13}C$ offset was -0.2 ± 0.4‰ for *Primnoa*, 0.0 ± 0.2‰ for *Isidella* and 0.2 ± 0.6‰ for *Kulamamana* (calculated as the average offset for all AAs analyzed, averaged across all individuals within a genus; Fig. 4). No individual AA $\delta^{13}C$ offsets between skeleton and polyp tissue were greater than 1‰, and only the non-essential AA Pro in *Primnoa* had a $\delta^{13}C$ offset that was significantly different from 0‰ (-1.0 ± 0.7‰; Table 1). As a result, the skeleton and polyp tissue from a single genus always clustered together in multivariate space (Fig. 3, Table C.5).

345 Using an AA isotope fingerprinting approach in a Bayesian stable isotope mixing model,
346 we compared estimates of the relative contribution of eukaryotic microalgae and prokaryotic
347 cyanobacteria to corals calculated from both tissues. The relative contribution results were very
348 similar whether we used the coral polyp tissue or the proteinaceous skeleton (Fig. 5). The mean
349 absolute value difference in relative contribution calculated from polyp vs. skeleton was 6 ± 3%
350 for *Primnoa*, 4 ± 2% for *Isidella*, and 5 ± 2% for *Kulamanamana* (calculated as the absolute
351 value of the difference in relative contribution for each end member between polyp tissue and
352 skeleton, averaged across all three end members for all individuals within a coral genera). This 4
353 to 6% variability between tissue types was within the variance in model output after 500,000
354 iterations of the SIAR mixing model (8 ± 1%).
355 We did find significant differences in the relative contribution of cyanobacteria-derived
356 carbon (One-way ANOVA, $F_{2,10} = 235.5$, $p = 3.9e^{-9}$) and eukaryotic microalgae-derived carbon
357 (One-way ANOVA, $F_{2,10} = 410.5$, $p = 2.5e^{-10}$) among the three corals (calculated from polyp
358 tissue, but the results were the same for skeleton). Both *Primnoa* from the Gulf of Alaska (77 ±
359 2%) and *Isidella* from the Central California Margin (68 ± 4%) relied heavily on export
360 production fueled by eukaryotic microalgae (Tukey's HSD, $p < 0.05$) (Fig. 5). Conversely,
361 *Kulamanamana* from the NPSG received relatively little input from eukaryotic microalgae (9 ±
362 5%) (Tukey's HSD, $p < 0.05$), instead receiving the majority of its carbon from cyanobacteria-
363 fixed carbon (74 ± 1%) (Tukey's HSD, $p < 0.05$) (Fig. 5). All three corals showed a small and
364 relatively consistent contribution of carbon from heterotrophic bacteria (12 ± 4% averaged across
365 all three genera) (Fig. 5).
366

3. 3 Amino acid nitrogen isotopes

As with carbon, individual AA $\delta^{15}N$ values differed significantly among the three coral genera (Fig. 6), with *Isidella* from the California Margin having the highest AA $\delta^{15}N$ values and *Kulamanamana* from the NPSG having the lowest AA $\delta^{15}N$ values. The trophic AAs were more positive than the source AAs, and Thr had the characteristically most negative $\delta^{15}N$ values.

$\delta^{15}N$ values did not differ significantly between coral skeleton and polyp tissue for any of the measurable source AAs: Phe (mean offset across all three genera = -0.1 ± 0.1‰), Lys (0.3 ± 0.1‰), and Met (0.1‰; however, Met was only present in sufficient quantity for analysis in *Primnoa*) (Fig. 7; Table 1). However, the mean offset in trophic AA $\delta^{15}N$ values between skeleton and polyp were significantly greater than 0‰ for all three genera: *Primnoa* = -2.8 ± 0.2‰ (one sample t-test, $t_4 = -32.4$, $p = 5.4e^{-6}$), *Isidella* = -3.5 ± 0.4‰ (one sample t-test, $t_4 = -22.0$, $p = 2.5e^{-5}$), and *Kulamanamana* = -3.2 ± 0.1‰ (one sample t-test, $t_2 = -56.8$, $p = 3.1e^{-4}$) (averaged across all trophic AAs within an individual and then averaged across all individuals within a genus) (Fig. 7). In particular, the mean offset for the canonical trophic AA Glu was remarkably consistent across all three coral genera: *Primnoa* = -3.4 ± 0.5‰, *Isidella* = -3.4 ± 0.5‰, and *Kulamanamana* = -3.4 ± 0.2‰ (averaged across individuals within a genus) (Fig. 7, Table 1). Thr $\delta^{15}N$ values were consistently offset between skeleton and polyp tissue for all three genera (mean offset across all three genera = 2.8 ± 0.6‰), but in the opposite direction as the trophic AAs (Fig. 7, Table 1). Gly and Ser had variable $\delta^{15}N$ offsets among the three genera though they were always closer to 0‰ than the trophic AAs and Thr (Fig. 7, Table 1).

All three coral genera had similar $TP_{CSI\text{-}AA}$ values when calculated from polyp tissue: *Primnoa* = 2.4 ± 0.2, *Isidella* = 2.4 ± 0.1, and *Kulamanamana* = 2.6 ± 0.1 (averaged across

individuals within a genus). However, given the large -3.4‰ offset in $\delta^{15}N$ value of Glu between skeleton and polyp tissue, coincident with no appreciable offset in Phe $\delta^{15}N$ value, $TP_{CSI\text{-}AA}$ estimates were nearly half a trophic level lower when calculated from skeleton AA $\delta^{15}N$ data, compared to estimates from polyp data. The mean $TP_{CSI\text{-}AA}$ offsets between skeleton and polyp were also very similar among genera: for *Primnoa* = -0.4 ± 0.1 (one sample t-test, $t_4 = -15.7$, $p = 9.5e^{-5}$), *Isidella* = -0.4 ± 0.1 (one sample t-test, $t_4 = -14.1$, $p = 1.5e^{-4}$), and *Kulamanamana* = -0.5 ± 0.1 (one sample t-test, $t_2 = -11.1$, $p = 0.008$).

4. DISCUSSION

Overall, the AA $\delta^{13}C$ and $\delta^{15}N$ offsets between coral polyp tissue and skeleton were consistent across three proteinaceous deep-sea coral genera. We found minimal offsets in the $\delta^{13}C$ values of both essential and non-essential AAs, as well as the $\delta^{15}N$ values of source AAs between polyp tissue and protein skeleton. However, the $\delta^{15}N$ values of trophic AAs in skeletal material were consistently 3-4‰ less than polyp tissue for all three genera. These observations suggest that these patterns of $\delta^{13}C$ and $\delta^{15}N$ offset between coral polyp tissue and proteinaceous skeleton are likely robust for gorgonin-based proteinaceous corals, linked to fundamental aspects of central metabolism and tissue synthesis. Our observations open the door for applying many of the rapidly evolving CSI-AA based tools developed for metabolically active tissues in modern systems to archival coral tissues in a paleoceanographic context.

4.1 Carbon isotopes

Amino acid carbon isotope fingerprinting has the potential to be used to reconstruct the main sources of primary production fueling consumers (e.g., Larsen et al. 2013; Arthur et al.

412 2014; McMahon et al. 2016). However, to apply this technique to paleoarchives, the $\delta^{13}C$ values
413 of individual AAs in archival structural tissues, such as proteinaceous skeletons, must accurately
414 reflect the $\delta^{13}C$ values of those same AAs in the metabolically active tissue. Our data showed
415 only small, non-systematic offsets in AA $\delta^{13}C$ values between coral polyp tissue and
416 proteinaceous skeleton. This observation indicates that deep-sea corals do not exhibit
417 substantially different carbon isotope fractionation of AAs during the synthesis of metabolically
418 active tissues and structural proteins from a shared dietary amino acid pool. As a result, we
419 conclude that information obtained from the $\delta^{13}C$ values of AAs in a proteinaceous coral
420 skeleton reflects the same information that would be obtained from the metabolically active
421 tissue. While the average offset in AA $\delta^{13}C$ value between tissues (averaged across all AAs) was
422 close to 0‰, there was notable variation about that mean $\delta^{13}C$ offset of individual AAs (typically
423 < 1‰) (Table 1). This variability likely reflects a combination of analytical uncertainty, small
424 offsets in the temporal window represented by the different integration times of polyp and
425 skeleton tissues, and potentially small differences in isotope fractionation during metabolism.
426 However, as noted in Section 2.2.2, our best estimate of the full intra-sample variability for
427 average $\delta^{13}C$ AA measurements using this protocol is ± 0.7‰. As such, differences in AA $\delta^{13}C$
428 values among samples likely cannot be reliably interpreted near or less than 0.7‰.
429 To our knowledge, there is only one prior study comparing AA $\delta^{13}C$ values in paired
430 metabolically active and bioarchival structural tissues (McMahon et al. 2011). In that study,
431 McMahon et al. (2011) found minimal offsets in AA $\delta^{13}C$ values between fish muscle and the
432 protein in biomineralized otoliths, which they similarly attributed to utilization of a shared amino
433 acid pool for biosynthesis of both tissue types. Taken together, our data suggest that the AA $\delta^{13}C$
434 values preserved in biomineralized tissues provide a faithful record of the AA $\delta^{13}C$ values of

435 metabolically active tissues across phylogenetically distant consumer taxa. However, it is
436 important to remember that given the differences in incorporation rates between coral polyps
437 (relatively fast) and proteinaceous skeleton (skeleton), corals that experience strong seasonal
438 changes in food source (sinking POM) could exhibit offsets in the geochemical signals recorded
439 in these two tissues.

440 One promising paleo-application for proteinaceous coral skeletons is using essential
441 amino acid $\delta^{13}C$ values within Bayesian mixing models to reconstruct past changes in algal
442 community composition supporting export production (e.g., Schiff et al. 2014; McMahon et al.
443 2015a). The central observation for our study's main question was that both living tissue (polyp)
444 and coral skeleton give identical (within error) estimates of different sources using this technique
445 (Fig. 5). This supports our original hypothesis that $\delta^{13}C$ AA fingerprinting approaches applied to
446 coral skeletons produce the same result as if those analyses were conducted on metabolically
447 active tissue integrating over the same time period.

448 While not the main focus of our study, our mixing model results of relative contribution
449 of prokaryotic cyanobacteria and eukaryotic microalgae fueling export production were
450 consistent with expectations based on phytoplankton community composition in the three
451 oceanographically distinct regions (Fig. 5). For example, both *Primnoa* from the Gulf of Alaska
452 and *Isidella* from the California Margin (77 ± 2% and 68 ± 4% respectively) relied heavily on
453 export production fueled by eukaryotic microalgae, as expected for these regions with strong
454 seasonal upwelling dominated by large eukaryotic phytoplankton (Chavez et al. 1991; Lehman
455 1996; Odate 1996; Strom et al. 2006). Conversely, *Kulamanamana* received the majority of their
456 essential AAs from cyanobacteria-fixed carbon (74 ± 1%), consistent with the cyanobacteria-
457 dominated plankton composition of the oligotrophic NPSG euphotic zone (Karl et al. 2001). Our

458 Bayesian mixing model results suggest that very little of the exported POM fed upon by any of
459 these proteinaceous deep-sea corals was derived from heterotrophic bacteria, consistent with past
460 estimates of direct heterotrophic bacterial contribution to sinking POM (Fuhrman 1992; Azam et
461 al. 1994; Wakeham 1995). Caution must be taken when interpreting small differences (<10%) in
462 relative contribution of end members, given the observed variability in AA $\delta^{13}C$ offset between
463 polyp and skeleton (Table 1), variability in the molecular isotopic training set (Table C.6), and
464 variance in the mixing output (± 8%). As such, the fact that the relative contribution results were
465 consistent between polyp tissue and protein skeleton within estimates of uncertainty supports our
466 hypothesis that the proteinaceous skeletons of deep-sea corals faithfully records the same
467 geochemical signals as metabolically active tissue over the same integration time.
468
469 **4.2 Nitrogen isotopes**
470 *4.2.1 Source AA $\delta^{15}N$ as a proxy for $\delta^{15}N_{baseline}$*
471 As we hypothesized, we found no significant offsets in source AA $\delta^{15}N$ values between
472 proteinaceous skeleton and polyp tissue for any of the coral genera in this study (Table 1). Since
473 source AA $\delta^{15}N$ values provide a robust proxy for $\delta^{15}N_{baseline}$ (reviewed in McMahon and
474 McCarthy 2016), these results provide strong validation for using source AA $\delta^{15}N$ values in
475 proteinaceous coral records to infer past changes in the sources and cycling of nitrogen fueling
476 export production (e.g. Sherwood et al. 2011, 2014). For instance, we found significant
477 differences in the $\delta^{15}N_{Phe}$ values among the three coral genera from oceanographically distinct
478 regions (Fig. 6), which were generally consistent with oceanographic regime. *Kulamanamana*
479 corals from the NPSG had the lowest source AA $\delta^{15}N$ values (2.6 ± 0.2‰), consistent with the
480 expected strong influence of ^{15}N-deplete nitrogen fixation in this region (Sherwood et al. 2014).

Conversely, *Primnoa* from the Gulf of Alaska ($\delta^{15}N_{Phe}$ = 7.3 ± 0.6‰) and *Isidella* from the California Margin ($\delta^{15}N_{Phe}$ = 10.0 ± 0.6‰) had more enriched $\delta^{15}N_{Phe}$ values, again consistent with the ^{15}N-enriched nitrate supporting these coastal eutrophic upwelling systems (Wu et al. 1997; Altabet et al. 1999; Voss et al. 2001; Collins et al. 2003). *Isidella*, in particular, had the highest source AA $\delta^{15}N$ values among the specimens. This likely reflects upwelling of ^{15}N-enriched nitrate transported from regions of strong denitrification in the Eastern Tropical North Pacific via the California Undercurrent (Vokhshoori and McCarthy 2014; Ruiz-Cooley et al., 2014).

4.2.2 Trophic AAs and TP_{CSI-AA}

Being able to estimate accurate TP_{CSI-AA} values in bioarchives is central to many CSI-AA paleoceanographic applications. TP_{CSI-AA} has been developed in coral records and sediments as a new proxy for tracking the trophic structure of planktonic ecosystems, which is likely tightly linked to overall nitrogen supply and nitricline depth (e.g., Sherwood et al. 2014; Batista et al. 2014). Measuring TP_{CSI-AA} in a paleorecord is also critical to determine the degree to which shifts in $\delta^{15}N$ values of exported POM over time are driven by shifts in planktonic ecosystem structure or "baseline" changes in the sources and cycling of nitrogen at the base of the food web (e.g. Batista et al., 2014).

We found a mean 3 to 4‰ offset in trophic AA $\delta^{15}N$ values between skeleton and polyp tissue (Fig. 7), which was in direct contrast to both our hypothesis and the widespread assumption of consistent trophic fractionation of AAs among tissues (McMahon and McCarthy 2016). Given the minimal offset in source AA $\delta^{15}N$ values between tissues, the estimated trophic position (TP_{CSI-AA}) of proteinaceous deep-sea coral from skeleton was approximately half a

trophic level lower than when $TP_{CSI\text{-}AA}$ was calculated from corresponding polyp tissue. The specific $TP_{CSI\text{-}AA}$ values calculated from coral skeleton using eq. 1 (mean 2.0 ± 0.1 across all three genera) also appear to be low based on expectations of POM feeding proteinaceous deep-sea corals. Direct $TP_{CSI\text{-}AA}$ estimates from sinking POM, for example, have generally indicated average TP values near 1.5 (e.g., McCarthy et al. 2007; Batista et al. 2014), leading to a general expectation that coral $TP_{CSI\text{-}AA}$ values should be near 2.5.

Our data indicate that a new correction factor (∂) is required for $TP_{CSI\text{-}AA}$ reconstructions from proteinaceous deep-sea coral skeletons, reflecting the observed offset in trophic AA $\delta^{15}N$ values between proteinaceous skeleton and polyp tissue. We propose a new $TP_{CSI\text{-}AA}$ equation for use with proteinaceous deep-sea coral skeletons:

$$TP_{CSI-AA-Skeleton} = 1 + \left[\frac{(\delta^{15}N_{Glu}+\partial)-\delta^{15}N_{Phe}-\beta}{TDF_{Glu-Phe}}\right] \quad (2)$$

which is modified from eq. 1 by the addition of a correction factor (∂). For deep-sea corals with gorgonin protein (e.g. *Primnoa, Isidella, Kulamanamana*), we found a remarkably consistent ∂ for Glu of 3.4 ± 0.1‰, which when applied to skeleton Glu $\delta^{15}N$ values in eq. 2, produced far more realistic $TP_{CSI\text{-}AA}$ estimates (2.5 ± 0.1). This means that prior $TP_{CSI\text{-}AA}$ values from deep-sea proteinaceous corals have likely been universally underestimated, however, it is important to note that comparisons of relative $TP_{CSI\text{-}AA}$ estimates using the same tissue type would not be affected by this correction factor.

4.2.3 Potential mechanisms for trophic AA $\delta^{15}N$ offsets

Our data bring up an important underlying mechanistic question: what is driving the consistent 3 to 4‰ offset in trophic AA $\delta^{15}N$ values between proteinaceous coral skeleton and metabolically active polyp tissue? The fact that we only observed $\delta^{15}N$ offsets for trophic AAs,

527 but not source AAs (Fig. 7) suggests that the underlying mechanism is related to differential
528 deamination/transamination during protein synthesis of these tissues. While confirming any
529 specific mechanism is beyond the scope of our data, the ^{15}N-depletetion of trophic AAs in
530 protein skeleton relative to metabolically active polyp tissue is most likely related to nitrogen
531 flux from central Glutamine/Glutamate pool (in our protocols measured as Glu) during tissue
532 synthesis.

533 The isotopic discrimination of AA nitrogen during metabolism is dependent on not only
534 the number and isotope effect of individual enzymatic reactions, but also on the turnover rate and
535 associated relative flux of nitrogen through those pathways (Fig. C.1; e.g., Handley and Raven
536 1992; Webb et al. 1998; Hayes 2001; Germain et al., 2013; Ohkouchi et al. 2015). For example,
537 rapid protein turnover in metabolically active tissues results in successive rounds of enzymatic
538 isotope discrimination, leading to higher tissue δ^{15}N values than in slow turnover tissues
539 (Waterlow 1981; Hobson et al. 1993, 1996; Schwamborn et al. 2002; Schmidt 2004). Therefore,
540 we hypothesize that the high protein turnover and enhanced nitrogen flux in the metabolically
541 active polyp tissue is likely linked to its ^{15}N-enrichment of trophic AAs compared to the slow
542 growing, non-turnover proteinaceous skeleton (Hawkins 1985; Houlihan 1991; Conceição 1997).
543 Because the exact biochemical pathways and associated isotope effects for the synthesis of polyp
544 tissue and skeleton AAs are not known, we cannot evaluate any more specific mechanistic
545 hypothesis. However, we suggest that understanding the relative nitrogen fluxes between the
546 static (accretionary) skeleton and the rapidly cycling polyp tissues, which continually exchanges
547 AA nitrogen with the central nitrogen pool, represents the most promising framework for future
548 research.

549 Interestingly, Thr also showed a consistent $\delta^{15}N$ offset between skeleton and polyp tissue
550 of a similar magnitude, but in the opposite direction, as the trophic AAs (Fig. 7). While the
551 underlying metabolic processes leading to Thr nitrogen isotope fractionation remain unclear,
552 multiple studies have noted a strong negative relationship between Thr and trophic AA nitrogen
553 isotope fractionation during trophic transfer (Bradley et al. 2015; McMahon et al. 2015b; Nielsen
554 et al. 2015; Mompeán et al. 2016). The consistent offset we observe does appear to be linked to
555 coral metabolism, and so its ecological implications for the use of $\delta^{15}N_{Thr}$ values may be a
556 valuable topic for further study.
557 Finally, we note that a temporal mismatch in the trophic structure of sinking POM
558 reflected in the short-term polyp tissue and longer-term skeleton (as has been suggested in the
559 literature for isotopic mismatches in bulk tissue e.g., Tieszen et al. 1983) cannot reasonably
560 explain the observed offsets in trophic AA $\delta^{15}N$ values. The AA $\delta^{15}N$ values of metabolically
561 active polyp tissue and archival protein skeleton should inherently reflect different temporal
562 integration windows, given the different incorporation rates of these tissues. However, it seems
563 extraordinarily unlikely that all corals in our study experienced the exact same shifts in trophic
564 position, both in magnitude and direction, despite being collected from very distinct
565 oceanographic regions (*Kulamanamana* from the NPSG, *Primnoa* from the Gulf of Alaska, and
566 *Isidella* from the California Margin) spanning a decade of time (*Kulamanamana* in 2004 and
567 2007, *Primnoa* in 2010 and 2013, and *Isidella* in 2014).
568
569 **5. CONCLUSIONS**
570 We found that the $\delta^{13}C$ values of AAs as well as the $\delta^{15}N$ values of source AAs preserved
571 in the proteinaceous skeletons of deep-sea gorgonin corals largely reflect the values recorded in

572 the metabolically active polyp tissue. However, we did observe an unexpected but remarkably
573 consistent $\delta^{15}N$ offset between trophic AAs in proteinaceous skeleton and metabolically active
574 polyp tissue, which must be accounted for via a correction factor (∂) when calculating coral
575 $TP_{CSI\text{-}AA}$ from proteinaceous skeletons. Future work will determine if the ∂ calculated in this
576 study applies to other proteinaceous structural tissues, such as chitonous *Antipathes* and
577 *Leiopathes* deep-sea corals, mollusk shells, and foraminifera tests, all of which can also provide
578 valuable high temporal resolution archives of past ocean conditions (Serban et al. 1988; Katz et
579 al. 2010; Prouty et al. 2014). Our results open the doors for applying many of the rapidly
580 evolving CSI-AA-based tools developed for metabolically active tissues in modern systems to
581 archival tissues in a paleoceanographic context.
582
583 **ACKNOWLEDGEMENTS**

584 We thank Peter Etnoyer for initiating the funded proposal for portions of this work and assisting
585 in the collection of Primnoa samples in the Gulf of Alaska. We thank the following captains and
586 crew of the following groups for boat logistics during sample collection: 1) the RV *Ka'imikai-o-*
587 *Kanaloa* and the Hawaii Undersea Research Lab's Pisces IV and V, 2) the Monterey Bay Area
588 Research Institute (MBARI) ROV Doc Ricketts, and 3) the H2000 ROV and FSV Alaska
589 Provider through Scripps University. We thank undergraduates at Claremont McKenna (S.
590 Barnes, D. Parks) and the University of California, Santa Cruz (J. Schiff, J. Liu) for assistance in
591 sample preparation and Dr. E. Gier for assistance in compound-specific data analysis. Dr. Paul
592 Koch (UCSC) provided input on hypotheses discussed in this paper. This work was supported by
593 the NOAA National Undersea Research Program: West Coast and Polar Region
594 (NA08OAR4300817) and the National Science foundation (OCE 1061689 and OCE 1635527).

A portion of this work was performed under the auspices of the U.S. Department of Energy by Lawrence Livermore National Laboratory under Contract DE-AC52-07NA27344.

REFERENCES

Altabet M. A., Pilskaln C., Thunell R., Pride C., Sigman D., Chavez F., and Francois R. (1999) The nitrogen isotope biogeochemistry of sinking particles from the margin of the eastern North Pacific. *Deep. Sea Res. Part I* **46**, 655–679.

Andrews A. H., Cordes E. E., Mahoney M. M., Munk K., Coale K. H., Cailliet G. M., and Heifetz J. (2002) Age, growth, and radiometric age validation of a deep-sea, habitat-forming gorgonian (*Primnoa resedaeformis*) from the Gulf of Alaska. *Hydrobiologia,* **471**, 101-110.

Arthur K. E., Kelez S., Larsen T., Choy C. A., and Popp B. N. (2014) Tracing the biosynthetic source of essential amino acids in marine turtles using δ13C fingerprints. *Ecology*,**95**, 1285-1293.

Azam F., Smith D. C., Steward G. F., and Hagström Å. (1994) Bacteria-organic matter coupling and its significance for oceanic carbon cycling. *Microb. Ecol.* **28**, 167-179.

Barker S., Cacho I., Benway H., and Tachikawa K. (2005) Planktonic foraminiferal Mg/Ca as a proxy for past oceanic temperatures: A methodological overview and data compilation for the Last Glacial Maximum. *Quat. Sci. Rev*. **24**, 821–834.

616 Batista F. C., Ravelo A. C., Crusius J., Casso M. A., and McCarthy M. D. (2014) Compound
617 specific amino acid $\delta^{15}N$ in marine sediments: A new approach for studies of the marine
618 nitrogen cycle. *Geochim. Cosmochim. Acta* **142**, 553–569.
619 Bligh E. G. and Dyer W. J. (1959) A rapid method of total lipid extraction and purification. *Can.*
620 *J. Biochem. Physiol*. **37**, 911–917.
621 Boecklen W. J., Yarnes C. T., Cook B. A. and James A. C. (2011) On the use of stable isotopes
622 in trophic ecology. *Annu. Rev. Ecol. Evol. Syst.* **42**, 411–440.
623 Bradley C. J., Wallsgrove N. J., Choy C. A., Drazen J. C., Hetherington E. D., Hoen D. K., and
624 Popp B. N. (2015) Trophic position estimates of marine teleosts using amino acid
625 compound specific isotopic analysis. *Limnol. Oceanogr* **13**, 476-493.
626 Braun A., Vikari A., Windisch W., and Auerswald K. (2014) Transamination governs nitrogen
627 isotope heterogeneity of amino acids in rats. *J. Agricult. Food Chem.* **62**, 8008-8013.
628 Bruland K. W., Rue E. L., and Smith G. J. (2001) Iron and macronutrients in California coastal
629 upwelling regimes: implications for diatom blooms. *Limnol. Oceanogr*. **46**, 1661–1674.
630 Cairns S. D. (2007). Deep-water corals: an overview with special reference to diversity and
631 distribution of deep-water scleractinian corals. *Bull. Mar. Sci.* **81**, 311-322.
632 Cairns S. D. and Bayer F. M. (2005) A review of the genus *Primnoa* (Octocorallia: Gorgonacea:
633 Primnoidae), with the description of two new species. *Bull. Mar. Sci.* **77**, 225–256.
634 Chavez F. P., Barber R. T., Kosro P. M., Huyer A., Ramp S. R., Stanton T. P., and Rojas de
635 Mendiola B. (1991) Horizontal transport and the distribution of nutrients in the coastal
636 transition zone off northern California: effects on primary production, phytoplankton
637 biomass and species composition. *J. Geophys. Res.* **96**, 14833-14848.

638 Chikaraishi Y., Kashiyama Y., Ogawa N. O., Kitazato H. and Ohkouchi N. (2007) Metabolic
639 control of nitrogen isotope composition of amine acids in macroalgae and gastropods:
640 implications for aquatic food web studies. *Mar. Ecol. Prog. Ser.* **342**, 85–90.
641 Chikaraishi Y., Ogawa N. O., Kashiyama Y., Takano Y., Suga H., Tomitani A., Miyashita H.,
642 Kitazato H. and Ohkouchi N. (2009) Determination of aquatic food-web structure based
643 on compound-specific nitrogen isotopic composition of amino acids. *Limnol. Oceanogr.*
644 **7**, 740–750.
645 Chikaraishi Y., Ogawa N. O., and Ohkouchi, N. (2010) Further evaluation of the trophic level
646 estimation based on nitrogen isotopic composition of amino acids. In *Earth, life, and*
647 *isotopes (eds.* N. Ohkouchi, I. Tayasu, and K. Koba). *Kyoto University Press,* Kyoto, pp.
648 37-51.
649 Chikaraishi Y., Steffan S. A., Ogawa N. O., Ishikawa N. F., Sasaki Y., Tsuchiya M., and
650 Ohkouchi N. (2014) High-resolution food webs based on nitrogen isotopic composition
651 of amino acids. *Ecology and Evolution* **4**, 2423–2449.
652 Childers A. R., Whitledge T. E. and Stockwell D. A. (2005) Seasonal and interannual variability
653 in the distribution of nutrients and chlorophyll a across the Gulf of Alaska shelf: 1998-
654 2000. *Deep Sea Res. Part II* **52**, 193–216.
655 Church M. J., Mahaffey C., Letelier R. M., Lukas R., Zehr J. P. and Karl D. M. (2009) Physical
656 forcing of nitrogen fixation and diazotroph community structure in the North Pacific
657 subtropical gyre. *Global Biogeochem. Cycles*, **23**.
658 Collins C. A., Pennington J. T., Castro C. G., Rago T. A. and Chavez F. P. (2003) The California
659 Current system off Monterey, California: Physical and biological coupling. *Deep Sea*
660 *Res. Part II* **50**, 2389–2404.

661 Conceição L. E. C., Van der Meeren T., Verreth J. A. J., Evjen M. S., Houlihan D. F. and Fyhn,
662 H. J. (1997) Amino acid metabolism and protein turnover in larval turbot (*Scophthalmus*
663 *maximus*) fed natural zooplankton or Artemia. *Mar. Biol.* **129**, 255-265.
664 Décima M., Landry M. R. and Popp B. N. (2013) Environmental perturbation effects on baseline
665 δ15N values and zooplankton trophic flexibility in the southern California Current
666 Ecosystem. *Limnol. Oceanogr.* **58**, 624–634.
667 Druffel E. R. M. (1997) Geochemistry of corals: Proxies of past ocean chemistry, ocean
668 circulation, and climate. *Proc. Natl. Acad. Sci.* **94**, 8354–8361.
669 Ehrlich H. (2010) *Biological materials of marine origin*. Springer, New York.
670 Eppley R. W., Sharp J. H., Renger E. H., Perry M. J., and Harrison W. G. (1977) Nitrogen
671 assimilation by phytoplankton and other microorganisms in the surface waters of the
672 central North Pacific *Oceanogr. Mar. Biol*. **39**, 111–120.
673 Fuhrman J. (1992) Bacterioplankton roles in cycling of organic matter: the microbial food web.
674 In *Primary productivity and biogeochemical cycles in the sea* (eds. P. G. Falkowski, A.
675 D. Woodhead, K. Vivirito). Springer, New York. pp. 361-383.
676 García-Reyes M. and Largier J. L. (2012) Seasonality of coastal upwelling off central and
677 northern California: New insights, including temporal and spatial variability. *J. Geophys.*
678 *Res. Ocean*. **117**, 1–17.
679 Germain L. R., Koch P. L., Harvey J., and McCarthy M. D. (2013) Nitrogen isotope
680 fractionation in amino acids from harbor seals: implications for compound-specific
681 trophic position calculations. *Mar. Ecol. Prog. Ser.* **482**, 265-277.
682 Goldberg W. M. (1974) Evidence of a sclerotized collagen from the skeleton of a gorgonian
683 coral. *Comp. Biochem. Physiol. Part B* **49**, 525–526.

684 Goodfriend G. A. (1997) Aspartic acid racemization and amino acid composition of the organic
685 endoskeleton of the deep-water colonial anemone Gerardia: Determination of longevity
686 from kinetic experiments. *Geochim. Cosmochim. Acta*, **61**, 1931-1939.
687 Gordon H. R. and Morel A. (1983) Remote assessment of ocean color for interpretation of
688 satellite visible imagery: a review. *Lect. Notes Coast. Estaur. Study* **4**, 1–114.
689 Gray D. (1857) Synopsis of the families and genera of axiferous zoophytes or barked corals.
690 *Proc. Zool. Soc. London* **25**, 1, 278-294.
691 Guilderson T. P., McCarthy M. D., Dunbar R. B., Englebrecht A, and Roark E. B. (2013) Late
692 Holocene variations in Pacific surface circulation and biogeochemistry inferred from
693 proteinaceous deep-sea corals. *Biogeosciences* **10**, 6019–6028.
694 Hamoutene D., Puestow T., Miller-Banoub J. and Wareham V. (2008) Main lipid classes in some
695 species of deep-sea corals in the Newfoundland and Labrador region (Northwest Atlantic
696 Ocean). *Coral Reefs* **27**, 237–246.
697 Handley L. L. and Raven J. A. (1992) The use of natural abundance of nitrogen isotopes in plant
698 physiology and ecology. *Plant Cell Environ.* **15**, 965–985.
699 Hare E. P., Fogel M. L., Stafford T. W., Mitchell A. D., and Hoering T. C. (1991) The isotopic
700 composition of carbon and nitrogen in individual amino acids isolated from modern and
701 fossil proteins. *J. Archaeol. Sci*. **18**, 277–292.
702 Hawkins A. J. S. (1985) Relationships between the synthesis and breakdown of protein, dietary
703 absorption and turnovers of nitrogen and carbon in the blue mussel, *Mytilus edulis* L.
704 *Oecologia* **66**, 42-49.
705 Hayes J. M. (2001) Fractionation of Carbon and Hydrogen Isotopes in Biosynthetic Processes.
706 *Rev. Mineral. Geochem.* **43**, 225–277.

Hebert C. E., Popp B. N., Fernie K. J., Ka'apu-Lyons C., Rattner B. A., and Wallsgrove N. (2016) Amino acid specific stable nitrogen isotope values in avian tissues: insights from captive American kestrels and wild herring gulls. *Environ. Sci. Technol.* **50**, 12928-12937.

Heikoop J. M., Hickmott D. D., Risk M. J., Shearer C. K. and Atudorei V. (2002) Potential climate signals from the deep-sea gorgonian coral *Primnoa resedaeformis*. *Hydrobiologia*, **471**, 117-124.

Henderson G. M. (2002) New oceanic proxies for paleoclimate. *Earth Planet. Sci. Lett*. **203**, 1–13.

Hill T. M., Myrvold C. R., Spero H. J. and Guilderson T. P. (2014) Evidence for benthic-pelagic food web coupling and carbon export from California margin bamboo coral archives. *Biogeosciences* **11**, 3845–3854.

Hobson K. A., Alisauskas R. T. and Clark R. G. (1993). Stable-nitrogen isotope enrichment in avian tissues due to fasting and nutritional stress: implications for isotopic analyses of diet. *Condor* 388-394.

Hobson K. A., Schell D. M., Renouf D., and Noseworthy E. (1996) Stable carbon and nitrogen isotopic fractionation between diet and tissues of captive seals: implications for dietary reconstructions involving marine mammals. *Can. J. Fish. Aquat. Sci.* **53**, 528–533.

Houlihan D. F. (1991). Protein turnover in ectotherms and its relationships to energetics. In *Advances in comparative and environmental physiology* (pp. 1-43). Springer Berlin Heidelberg.

Howland M. R., Corr L. T., Young S. M. M., Jones V., Jim S., Van Der Merwe N. J., Mitchell A. D. and Evershed R. P. (2003) Expression of the dietary isotope signal in the compound-

specific δ13C values of pig bone lipids and amino acids. *Int. J. Osteoarchaeol*. **13**, 54–65.

Hutchins D. A. and Bruland K. W. (1998). Iron-limited diatom growth and Si: N uptake ratios in a coastal upwelling regime. *Nature* **393**, 561-564.

Karl D. M., Bidigare R. R., and Letelier R. M. (2001) Long-term changes in plankton community structure and productivity in the North Pacific Subtropical Gyre: The domain shift hypothesis. *Deep Sea Res. Part II* **48**, 1449–1470.

Karl D. M., Bidigare R. R., Church M. J., Dore J. E., Letelier R. M., Mahaffey C., and Zehr J. P. (2008) The nitrogen cycle in the North Pacific trades biome: an evolving paradigm. *Nitro. Mar. Environ.* **2**, 705-769.

Katz M. E., Cramer B. S., Franzese A., Honisch B., Miller K. G., Rosenthal Y., and Wright J. D. (2010) Traditional and Emerging Geochemical Proxies in Foraminifera. *J. Foraminifer. Res*. **40**, 165–192.

Ladd C., Stabeno P., and Cokelet E. D. (2005). A note on cross-shelf exchange in the northern Gulf of Alaska. *Deep Sea Ress Part II* **52**, 667-679.

Larsen T., Taylor D. L., Leigh M. B., and O'Brien D. M. (2009) Stable isotope fingerprinting: a novel method for identifying plant, fungal, or bacterial origins of amino acids. *Ecology* **90**, 3526–35.

Larsen T., Ventura M., Andersen N., O'Brien D. M., Piatkowski U., and McCarthy M. D. (2013) Tracing carbon sources through aquatic and terrestrial food webs using amino acid stable isotope fingerprinting. *PLoS One* **8**, e73441.

Larsen T., Bach L. T. Salvatteci R., Wang Y. V., Andersen N., Ventura M., and McCarthy M. D. (2015) Assessing the potential of amino acid patterns as a carbon source tracer in marine

753 sediments: effects of algal growth conditions and sedimentary diagenesis.
754 *Biogeosciences*, **12**, 4979-4992.
755 Lee T. N., Buck C. L., Barnes B. M., and O'Brien D. M. (2012) A test of alternative models for
756 increased tissue nitrogen isotope ratios during fasting in hibernating arctic ground
757 squirrels. *J. Exp. Biol.* **215**, 3354-3361.
758 Lehman J. (2009) Compound-specific amino acid isotopes as tracers of algal central metabolism:
759 developing new tools for tracing prokaryotic vs. eukaryotic primary production and
760 organic nitrogen in the ocean MS thesis, University of California, Santa Cruz
761 Lehman P. W. (1996) Changes in chlorophyll a concentration and phytoplankton community
762 composition with water-year type in the upper San Francisco Bay Estuary. *San Francisco*
763 *Bay: The Ecosystem. Pac. Div. Am. Assoc. Adv. Sc.* 351-374.
764 Lehmann M. F., Bernasconi S. M., Barbieri A. and McKenzie J. A. (2002) Preservation of
765 organic matter and alteration of its carbon and nitrogen isotope composition during
766 simulated and in situ early sedimentary diagenesis. *Geochim. Cosmochim. Acta* **66**,
767 3573–3584.
768 Lorrain A., Graham B. S., Popp B. N., Allain V., Olson R. J., Hunt B. P., Fry B., Galván-Magaña
769 F., Menkes C. E. R., Kaehler S., and Ménard F. (2015) Nitrogen isotopic baselines and
770 implications for estimating foraging habitat and trophic position of yellowfin tuna in the
771 Indian and Pacific Oceans. *Deep Sea Res. Part II*, **113**, 188-198.
772 McCarthy M. D., Benner R., Lee C., and Fogel M. L. (2007) Amino acid nitrogen isotopic
773 fractionation patterns as indicators of heterotrophy in plankton, particulate, and dissolved
774 organic matter. *Geochim. Cosmochim. Acta* **71**, 4727–4744.

McCarthy M. D., Lehman J., and Kudela R. (2013) Compound-specific amino acid $\delta^{15}N$ patterns in marine algae: tracer potential for cyanobacterial vs. eukaryotic organic nitrogen sources in the ocean. *Geochim. Cosmochim. Acta* **103**, 104–120.

McClelland J. and Montoya J. (2002) Trophic relationships and the nitrogen isotopic composition of amino acids in plankton. *Ecology* **83**, 2173–2180.

McMahon K. W. and McCarthy M. D. (2016) Embracing variability in amino acid $\delta^{15}N$ fractionation: mechanisms, implications, and applications for trophic ecology. *Ecosphere* **7**, 1-26.

McMahon K. W., Fogel M. L., Elsdon T. S., and Thorrold S. R. (2010) Carbon isotope fractionation of amino acids in fish muscle reflects biosynthesis and isotopic routing from dietary protein. *J. Anim. Ecol.* **79**, 1132–1141.

McMahon K. W., Berumen M. L., Mateo I., Elsdon T. S., and Thorrold S. R. (2011) Carbon isotopes in otolith amino acids identify residency of juvenile snapper (Family: Lutjanidae) in coastal nurseries. *Coral Reefs* **30**, 1135–1145.

McMahon K. W., McCarthy M. D., Sherwood O. A., Larsen T., and Guilderson T. P. (2015a). Millennial-scale plankton regime shifts in the subtropical North Pacific Ocean. *Science* **350**, 1530-1533.

McMahon K. W., Thorrold S. R., Elsdon T. S., and McCarthy M. D. (2015b) Trophic discrimination of nitrogen stable isotopes in amino acids varies with diet quality in a marine fish. *Limnol. Oceanogr.* **60**, 1076-1087.

McMahon K. W., Thorrold S. R., Houghton L. A., and Berumen M. L. (2016) Tracing carbon flow through coral reef food webs using a compound-specific stable isotope approach. *Oecologia* **180**, 809-821.

798 Meyers P. A. (1994) Preservation of elemental and isotopic source identification of sedimentary
799 organic matter. *Chem. Geol*. **114**, 289–302.
800 Mompeán C., Bode A., Gier E., and McCarthy, M. D. (2016) Bulk vs. amino acid stable nitrogen
801 isotope estimations of metabolic status and contributions of nitrogen fixation to size-
802 fractionated zooplankton biomass in the subtropical North Atlantic. *Deep Sea Res. Part I*.
803 **114**, 137-148
804 Nielsen J. M. and Winder M. (2015) Seasonal dynamics of zooplankton resource use revealed by
805 carbon amino acid stable isotope values. *Mar. Ecol. Prog. Ser.* **531**, 143–154.
806 Nielsen J. M., Popp B. N., and Winder M. (2015) Meta-analysis of amino acid stable nitrogen
807 isotope ratios for estimating trophic position in marine organisms. *Oecologia*, **178**, 631-
808 642.
809 Odate T. (1996) Abundance and size composition of the summer phytoplankton communities in
810 the western North Pacific Ocean, the Bering Sea, and the Gulf of Alaska. *J. Oceanogr.*
811 **52**, 335-351.
812 Ohkouchi N., Chikaraishi Y., Close H. G., Fry B., Larsen T., Madigan D. J., McCarthy M. D.,
813 McMahon K. W., Nagata T., Naito Y. I., Ogawa N. O., Popp B. N., Steffan S., Takano
814 Y., Tayasu I., Wyatt A. S. J., Yamaguchi Y. T., Yokoyama Y. (2017). Advances in the
815 application of amino acid nitrogen isotopic analysis in ecological and biogeochemical
816 studies. *Org. Geochem*. DOI:10.1016/j.orggeochem.2017.07.009
817 Ohkouchi N., Ogawa N. O., Chikaraishi Y., Tanaka H. and Wada E. (2015) Biochemical and
818 physiological bases for the use of carbon and nitrogen isotopes in environmental and
819 ecological studies. *Prog. Earth Planet. Sci.* **2**, 1–17.

820 Orejas C., Gili J., and Arntz W. (2003) The role of the small planktonic communities in the diet
821 of two Antarctic octocorals (*Primnoisis antarctica* and *Primnoella sp*.). *Mar. Ecol. Prog.*
822 *Ser.* **250**, 105–116.
823 Parnell A. C., Inger R., Bearhop S. and Jackson A. L. (2010) Source Partitioning Using Stable
824 Isotopes: Coping with Too Much Variation. *PLoS One* **5**, e9672.
825 Parrish F. A. (2015) Settlement, colonization, and succession patterns of gold coral
826 *Kulamanamana haumeaae* in Hawaiian deep coral assemblages. *Mar. Ecol. Prog. Ser.*
827 **533**, 135–147.
828 Popp B. N., Graham B. S., Olson R. J., Hannides C. C. S., Lott M. J., López-Ibarra G. A.,
829 Galván-Magaña F., and Fry B. (2007) Insight into the trophic ecology of yellowfin tuna,
830 *Thunnus albacares*, from compound-specific nitrogen isotope analysis of proteinaceous
831 amino acids. *Terr. Ecol.* **1**, 173–190.
832 Post D. M. (2002) Using stable isotopes to estimate trophic position: models, methods, and
833 assumptions. *Ecology* **83**, 703–718.
834 Prouty N. G., Roark E. B., Koenig A. E., Demopoulos A. W., Batista F. C., Kocar B. D., Selby
835 D., and Ross S. W. (2014) Deep‐sea coral record of human impact on watershed quality
836 in the Mississippi River Basin. *Global Biogeochem. Cycles*, **28**, 29-43.
837 R Core Team (2013) R: A language and environment for statistical computing. R Foundation for
838 Statistical Computing, Vienna, Austria. http://www.R-project.org/.
839 Reeds P. J. (2000) Dispensable and indispensable amino acids for humans. *J. Nutr.* **130**, 1835S–
840 40S.

841 Ribes M., Coma R., and Gili J. M. (1999) Heterogeneous feeding in benthic suspension feeders:
842 The natural diet and grazing rate of the temperate gorgonian *Paramuricea clavata*
843 (Cnidaria: Octocorallia) over a year cycle. *Mar. Ecol. Prog. Ser.* **183**, 125–137.
844 Risk M. J., Heikoop J. M., Snow M. G., and Beukens R. (2002) Lifespans and growth patterns of
845 two deep-sea corals: *Primnoa resedaeformis* and *Desmophyllum cristagalli*.
846 *Hydrobiologia,* **471**, 125-131.
847 Roark E. B., Guilderson T. P., Flood-Page S., Dunbar R. B., Ingram B. L., Fallon S. J., and
848 McCulloch M. (2005) Radiocarbon-based ages and growth rates of bamboo corals from
849 the Gulf of Alaska. *Geophys. Res. Lett.* **32**, 1–5.
850 Roark E. B., Guilderson T. P., Dunbar R. B., and Ingram B. L. (2006) Radiocarbon-based ages
851 and growth rates of Hawaiian deep-sea corals. *Mar. Ecol. Prog. Ser*. **327**, 1–14.
852 Roark E. B., Guilderson T. P., Dunbar R. B., Fallon S. J., and Mucciarone D. A. (2009) Extreme
853 longevity in proteinaceous deep-sea corals. *Proc. Natl. Acad. Sci.* **106**, 5204–5208.
854 Roberts S. and Hirshfield M. (2004) Deep-sea corals: out of sight, but no longer out of mind.
855 *Front. Ecol. Environ.* **2**, 123–130.
856 Robinson L. F., Adkins J. F., Frank N., Gagnon A. C., Prouty N. G., Brendan Roark E., and de
857 Flierdt T. van (2014) The geochemistry of deep-sea coral skeletons: A review of vital
858 effects and applications for palaeoceanography. *Deep. Res. Part II* **99**, 184–198.
859 Rothwell R. G. and Rack F. R. (2006) New techniques in sediment core analysis: an
860 introduction. *Geol. Soc. London, Spec. Publ.* **267**, 1–29.
861 Ruiz-Cooley R. I., Koch P. L., Fiedler P. C., and McCarthy M. D. (2014) Carbon and nitrogen
862 isotopes from top predator amino acids reveal rapidly shifting ocean biochemistry in the
863 Outer California Current. *PloS one*. **9**, e110355.

Sambrotto R. N., and Lorenzen C. J. (1986) Phytoplankton and primary production. In *The Gulf of Alaska: physical environment and biological resources* (eds. D. W. Hood and S. T. Zimmerman). US Department of Commerce, Washington, DC, pp. 249–282.

Schiff J. T., Batista F. C., Sherwood O. a., Guilderson T. P., Hill T. M., Ravelo A. C., McMahon K. W., and McCarthy M. D. (2014) Compound specific amino acid $\delta^{13}C$ patterns in a deep-sea proteinaceous coral: Implications for reconstructing detailed $\delta^{13}C$ records of exported primary production. *Mar. Chem*. **166**, 82–91.

Schmidt K., McClelland J. W., Mente E., Montoya J. P., Atkinson A., and Voss M. (2004) Trophic-level interpretation based on $\delta^{15}N$ values: implications of tissue-specific fractionation and amino acid composition. *Mar. Ecol. Prog. Ser.* **266**, 43–58.

Schwamborn R., Ekau W., Voss M. and Saint-Paul U. (2002) How important are mangroves as a carbon source for decapod crustacean larvae in a tropical estuary? *Mar. Ecol. Prog. Ser.* **229**, 195-205.

Scott J. H., O'Brien D. M., Emerson D., Sun H., McDonald G. D., Salgado A., and Fogel M. L. (2006) An examination of the carbon isotope effects associated with amino acid biosynthesis. *Astrobiology* **6**, 867–880.

Serban A., Engel M. H. and Macko S. A. (1988) The distribution, stereochemistry and stable isotopic composition of amino acid constituents of fossil and modern mollusk shells. *Org. Geochem*. **13**, 1123–1129.

Sherwood O. A. and Edinger E. N. (2009) Ages and growth rates of some deep-sea gorgonian and antipatharian corals of Newfoundland and Labrador. *Can. J. Fish. Aquat. Sci.* **66**, 142–152.

886 Sherwood O. A., Scott D. B., Risk M. J. and Guilderson T. P. (2005) Radiocarbon evidence for
887 annual growth rings in the deep-sea octocoral *Primnoa resedaeformis*. *Mar. Ecol. Prog.*
888 *Ser*. **301**, 129–134.
889 Sherwood O. A., Thresher R. E., Fallon S. J., Davies D. M., and Trull T. W. (2009) Multi-
890 century time-series of ^{15}N and ^{14}C in bamboo corals from deep Tasmanian seamounts:
891 evidence for stable oceanographic conditions. *Mar. Ecol. Prog. Ser.* **397**, 209–218.
892 Sherwood O. A., Lehmann M. F., Schubert C. J., Scott D. B. and McCarthy M. D. (2011)
893 Nutrient regime shift in the western North Atlantic indicated by compound-specific $\delta^{15}N$
894 of deep-sea gorgonian corals. *Proc. Natl. Acad. Sci.* **108**, 1011–1015.
895 Sherwood O. A., Guilderson T. P., Batista F. C., Schiff J. T., and McCarthy M. D. (2014)
896 Increasing subtropical North Pacific Ocean nitrogen fixation since the Little Ice Age.
897 *Nature* **505**, 78–81.
898 Silfer J. A., Engel M. H., Macko S. A., and Jumeau E. J. (1991) Stable carbon isotope analysis of
899 amino acid enantiomers by conventional isotope ratio mass spectrometry and combined
900 gas chromatography/isotope ratio mass spectrometry. *Anal. Chem*. **63**, 370–374.
901 Sinniger F., Ocana O. V., and Baco A. R. (2013). Diversity of zoanthids (Anthozoa:
902 Hexacorallia) on Hawaiian seamounts: description of the Hawaiian gold coral and
903 additional zoanthids. *PloS one*, **8**, e52607.
904 Strom S. L., Olson M. B., Macri E. L., and Mordy C. W. (2006) Cross-shelf gradients in
905 phytoplankton community structure, nutrient utilization, and growth rate in the coastal
906 Gulf of Alaska. *Mar. Ecol. Prog. Ser*. **328**, 75–92.

907 Strub P. T., Allen J. S., Huyer A., Smith R. L., and Beaedsley R. C. (1987) Seasonal cycles of
908 currents, temperatures, winds, and sea level over the northeast pacific continental shelf:
909 35N to 48N. *J. Geophys. Res. Ocean.* **92**, 1507–1526.
910 Strzepek K. M., Thresher R. E., Revill A. T., Smith C. I., Komugabe A. F., and Fallon S. F.
911 (2014) Preservation effects on the isotopic and elemental composition of skeletal
912 structures in the deep-sea bamboo coral *Lepidisis spp.* (Isididae). *Deep. Res. Part II* **99**,
913 199–206.
914 Takizawa Y. and Chikaraishi Y. (2014). Are baby sprouts eating the proteins in the mother sweet
915 potato? *Researches in Organic Geochemistry* **30**, 29–32.
916 Thresher R., Rintoul S. R., Koslow J. A, Weidman C., Adkins J., and Proctor C. (2004) Oceanic
917 evidence of climate change in southern Australia over the last three centuries. *Geophys.*
918 *Res. Lett*. **31**, 2–5.
919 Tieszen L. L., Boutton T. W., Tesdahl K. G. and Slade, N. A. (1983). Fractionation and turnover
920 of stable carbon isotopes in animal tissues: implications for $\delta^{13}C$ analysis of diet.
921 *Oecologia*, **57**, 32-37.
922 Ueda K., Morgan S. L., Fox A., Gilbart J., Sonesson A., Larsson L., and Odham G. (1989) D-
923 alanine as a chemical marker for the determination of streptococcal cell wall levels in
924 mammalian tissues by gas chromatography/negative ion chemical ionization mass
925 spectrometry. *Anal. Chem.* **61**, 265-270.
926 Vokhshoori N. L. and McCarthy M. D. (2014) Compound-specific $\delta^{15}N$ amino acid
927 measurements in littoral mussels in the California upwelling ecosystem: a new approach
928 to generating baseline $\delta^{15}N$ isoscapes for coastal ecosystems. *PloS one*, **9**, e98087.

929 Voss M., Dippner J. W., and Montoya J. P. (2001) Nitrogen isotope patterns in the oxygen-
930 deficient waters of the Eastern Tropical North Pacific Ocean. *Deep. Res. Part I* **48**, 1905–
931 1921.
932 Wada E., Mizutani H., and Minagawa M. (1991) The use of stable isotopes for food web
933 analysis. *Crit. Rev. Food Sci. Nut*r. **30**, 361–71.
934 Wakeham S. G. (1995) Lipid biomarkers for heterotrophic alteration of suspended particulate
935 organic matter in oxygenated and anoxic water columns of the ocean. *Deep Sea Res. Part*
936 *I* **42**, 1749-1771.
937 Wakeham S. G. and Lee C. (1989) Organic geochemistry of particulate matter in the ocean: the
938 role of particles in oceanic sedimentary cycles. *Org. Geochem*. **14**, 83–96.
939 Walker B. D. and McCarthy M. D. (2012) Elemental and isotopic characterization of dissolved
940 and particulate organic matter in a unique California upwelling system: importance of
941 size and composition in the export of labile material. *Limnol. Oceanogr*. **57**, 1757–1774.
942 Ward E. J., Semmens B. X., and Schindler D. E. (2010) Including source uncertainty and prior
943 information in the analysis of stable isotope mixing models. *Environ. Sci. Technol*. **44**,
944 4645–4650.
945 Waterlow, J. C. (1981) N end-product methods for the study of whole body protein turnover.
946 *Proc. Nutr. Soc*. **40**, 317-320.
947 Webb S., Hedges R., and Simpson S. (1998) Diet quality influences the $\delta^{13}C$ and $\delta^{15}N$ of locusts
948 and their biochemical components. *J. Exp. Biol.* **201**, 2903–2911.
949 Williams B., Risk M., Stone R., Sinclair D., and Ghaleb B. (2007) Oceanographic changes in the
950 North Pacific Ocean over the past century recorded in deep-water gorgonian corals. *Mar.*
951 *Ecol. Prog. Ser*. **335**, 85–94.

Williams B., Thibodeau B., Chikaraishi Y., Ohkouchi N., Walnum A., Grottoli A., and Colin P. (2016) Consistency in coral skeletal amino acid composition offshore of Palau in the western Pacific warm pool indicates no impact of decadal variability in nitricline depth on primary productivity. *Limnol. Oceanogr.* **62**, 399-407.

Wu J., Calvert S. E., and Wong C. S. (1997) Nitrogen isotope variations in the subarctic northeast Pacific: relationships to nitrate utilization and trophic structure. *Deep. Res. Part I* **44**, 287–314.

TABLES

Table 1. Mean (‰ ± SD) offset (skeleton minus polyp tissue) of individual amino acid $\delta^{13}C$ and $\delta^{15}N$ values for three genera of proteinaceous deep-sea coral. One sample t-tests determined if mean offsets were significantly different from 0‰ (t statistic [df = 4 for *Primnoa* and *Isidella*, df = 2 for *Kulamanamana*] $^{ns}p > 0.05$, $*p < 0.05$, $**p < 0.01$, $***p < 0.001$). Amino acid names are in conventional three-letter abbreviation format. Essential and non-essential amino acids designated with ^{E} and ^{N}, respectively; trophic and source amino acids designated with ^{T} and ^{S}, respectively; amino acids with poorly characterized fractionation during trophic transfer designated with $^{?}$. na = not analyzed.

	Primnoa pacifica		*Isidella sp.*		*Kulamanamana haumeaae*	
	$\delta^{13}C$ (‰)	$\delta^{15}N$ (‰)	$\delta^{13}C$ (‰)	$\delta^{15}N$ (‰)	$\delta^{13}C$ (‰)	$\delta^{15}N$ (‰)
$Ala^{N,T}$	-0.1 ± 0.8 (-0.13^{ns})	-3.1 ± 0.5 (-15.42***)	-0.2 ± 0.8 (-0.49^{ns})	-3.8 ± 0.7 (-12.90***)	-0.9 ± 0.5 (-2.90^{ns})	-3.4 ± 0.4 (-13.78**)
$Asp^{N,T}$	-0.1 ± 0.5 (-0.59^{ns})	-3.2 ± 0.3 (-20.53***)	-0.2 ± 0.8 (-0.70^{ns})	-3.8 ± 0.6 (-15.28***)	0.8 ± 0.6 (2.21^{ns})	-3.1 ± 0.3 (-21.03**)
$Glu^{N,T}$	-0.3 ± 0.6 (-1.10^{ns})	-3.4 ± 0.5 (-16.26***)	-0.2 ± 0.5 (-0.90^{ns})	-3.4 ± 0.5 (-15.50***)	0.7 ± 0.5 (2.16^{ns})	-3.4 ± 0.2 (-37.02***)
$Gly^{N,?}$	-0.3 ± 0.4 (-1.56^{ns})	0.7 ± 0.3 (5.35^{ns})	0.2 ± 0.5 (1.10^{ns})	1.3 ± 0.3 (9.79***)	0.9 ± 0.5 (3.41^{ns})	0.8 ± 0.3 (4.79*)
$Ile^{E,T}$	0.1 ± 0.6 (0.39^{ns})	-2.3 ± 0.3 (-15.02***)	0.2 ± 0.8 (0.59^{ns})	-3.6 ± 0.4 (-21.26***)	0.2 ± 0.2 (2.05^{ns})	-3.3 ± 0.3 (-16.70**)
$Leu^{E,T}$	0.3 ± 0.6 (1.06^{ns})	-2.9 ± 0.6 (-11.39***)	-0.2 ± 0.3 (-1.84^{ns})	-3.8 ± 0.7 (-12.26***)	-0.3 ± 0.5 (-1.08^{ns})	-3.4 ± 0.2 (-26.40**)
$Lys^{E,S}$	na	0.3 ± 0.6 (1.05^{ns})	na	0.3 ± 0.4 (1.89^{ns})	na	0.2 ± 0.2 (1.77^{ns})
$Met^{E,S}$	na	0.1 ± 0.6 (0.54^{ns})	na	na	na	na
$Phe^{E,S}$	-0.2 ± 0.6 (-0.90^{ns})	-0.1 ± 0.3 (-0.42^{ns})	0.2 ± 0.5 (0.72^{ns})	-0.2 ± 0.2 (-2.36^{ns})	0.5 ± 0.8 (1.05^{ns})	-0.0 ± 0.4 (0.16^{ns})
$Pro^{N,T}$	-1.0 ± 0.7 (-3.03*)	-2.9 ± 0.5 (-13.89***)	-0.0 ± 0.5 (0.08^{ns})	-3.9 ± 0.2 (-37.02***)	0.3 ± 1.2 (0.47^{ns})	-3.3 ± 0.3 (-20.09**)
$Ser^{N,?}$	-0.0 ± 0.8 (0.02^{ns})	0.4 ± 0.7 (1.39^{ns})	-0.0 ± 0.7 (-0.13^{ns})	0.7 ± 0.3 (4.62**)	0.6 ± 1.0 (1.02^{ns})	0.3 ± 0.4 (1.33^{ns})
$Thr^{E,?}$	-0.5 ± 0.7 (-1.65^{ns})	3.4 ± 0.5 (16.72***)	0.3 ± 0.4 (1.97^{ns})	2.5 ± 0.6 (9.83***)	0.6 ± 0.3 (2.85^{ns})	2.4 ± 0.3 (15.33**)
$Val^{E,T}$	0.2 ± 0.6 (0.63^{ns})	-1.9 ± 0.4 (-10.45***)	0.2 ± 0.4 (0.87^{ns})	-2.2 ± 0.7 (-7.13**)	-0.8 ± 0.9 (-1.64^{ns})	-2.3 ± 0.3 (-14.53**)

984 **FIGURE CAPTIONS**

985 Figure 1. Collection sites and deep-sea coral genera. Collection information for three genera of
986 proteinaceous deep-sea coral, *Primnoa pacifica* (square symbols, n = 5) from the coastal region
987 of the Gulf of Alaska, *Isidella sp.* (triangle symbols, n = 5) from Sur Ridge in the Central
988 California Margin, and *Kulamanamana haumeaae* (circle symbols, n = 3) from the Hawaiian
989 Archipelago in the North Pacific Subtropical Gyre. Color contours reflect remote sensing-
990 derived chlorophyll a concentrations for the North Pacific from SeaWiFS seasonal climatology
991 for the boreal spring 1998-2010 (image courtesy of Norman Kuring of the Ocean Biology
992 Processing Group NASA/GSFC). Inset photos show the living coral structure and proteinaceous
993 skeleton cross sections (enlarged Fig. A.1): A) *Primnoa* colony (Photo credit: Ocean Networks
994 Canada), B) *Primnoa* cross-section (B. Williams Lab), C) *Isidella* colony (NOAA Office of
995 Ocean Exploration), D) *Isidella* cross-section (M. McCarthy Lab), E) *Kulamanamana* colony
996 (Sinniger et al. 2013), F) *Kulamanama* cross-section (Sherwood et al. 2014).

997 Figure 2. Coral amino acid $\delta^{13}C$ values. Mean individual amino acid $\delta^{13}C$ values (‰ ± SD) in
998 polyp tissue (filled symbols) and proteinaceous skeleton (open symbols) from three genera of
999 proteinaceous deep-sea coral: *Primnoa pacifica* (cyan squares, n = 5), *Isidella sp.* (magenta
1000 triangles, n = 5), and *Kulamanamana haumeaae* (green circles, n = 3).

1001 Figure 3. Principal component analysis of eleven coral amino acid $\delta^{13}C$ values from polyp
1002 tissues (filled symbols) and proteinaceous skeleton (open symbols) of three genera of deep-sea
1003 corals: *Primnoa pacifica* (n = 5 individual colonies) from the Gulf of Alaska, *Isidella sp.* (n = 5
1004 individual colonies) from the Central California Margin, and *Kulamanamana haumeaae* (n = 3
1005 individual colonies) from the North Pacific Subtropical Gyre. Variance of principal components
1006 is in parentheses on each axis (Table C.5). Loadings of the eleven amino acids (conventional

three-letter abbreviation format) are shown as arrows from the center (Table C.5).

Figure 4. Coral amino acid $\delta^{13}C$ offsets between tissues. Mean (‰ ± SD) individual amino acid $\delta^{13}C$ offset (proteinaceous skeleton minus polyp tissue) from three genera of proteinaceous deep-sea coral: *Primnoa pacifica* (cyan squares, n = 5), *Isidella sp.* (magenta triangles, n = 5), and *Kulamanamana haumeaae* (green circles, n = 3).

Figure 5. Comparison of amino acid $\delta^{13}C$ fingerprinting estimates of exported plankton composition. Relative contribution of carbon from prokaryotic cyanobacteria (dark blue), eukaryotic microalgae (green), and heterotrophic bacteria (black) to three genera of proteinaceous deep-sea coral: *Primnoa pacifica* (n = 5), *Isidella sp.* (n = 5), and *Kulamanamana haumeaae* (n = 3) as calculated from polyp tissue (filled bars) and proteinaceous skeleton (open bars). Relative contributions were calculated using an amino acid fingerprinting approach in a fully Bayesian stable isotope mixing model framework using the normalized $\delta^{13}C$ values of five essential amino acids (Thr, Ile, Val, Phe, Leu) from published plankton end-members and deep-sea coral tissues.

Figure 6. Coral amino acid $\delta^{15}N$ values. Mean individual amino acid $\delta^{15}N$ values (‰ ± SD) in polyp tissue (filled symbols) and proteinaceous skeleton (open symbols) from three genera of proteinaceous deep-sea coral: *Primnoa pacifica* (cyan squares, n = 5), *Isidella sp.* (magenta triangles, n = 5), and *Kulamanamana haumeaae* (green circles, n = 3).

Figure 7. Coral amino acid $\delta^{15}N$ offsets between tissues. Mean (‰ ± SD) individual amino acid $\delta^{15}N$ offset (proteinaceous skeleton minus polyp tissue) from three genera of proteinaceous deep-sea coral: *Primnoa pacifica* (cyan squares, n = 5), *Isidella sp.* (magenta triangles, n = 5), and *Kulamanamana haumeaae* (green circles, n = 3).

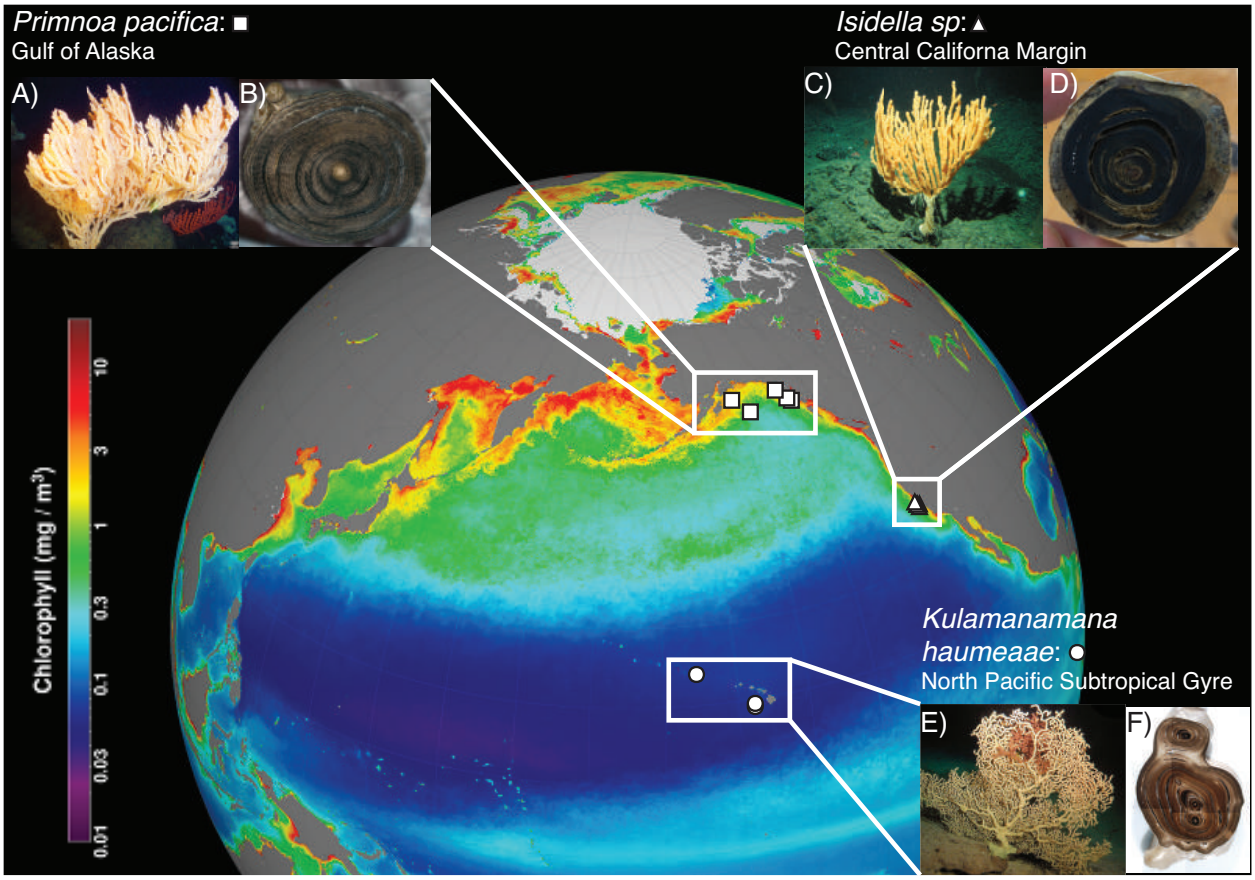
Primnoa pacifica: ■
Gulf of Alaska
A)
B)
Isidella sp: ▲
Central California Margin
C)
D)
Chlorophyll (mg / m³)
10
3
1
0.3
0.1
0.03
0.01
Kulamanamana haumeaae: ○
North Pacific Subtropical Gyre
E)
F)

Figure 1.

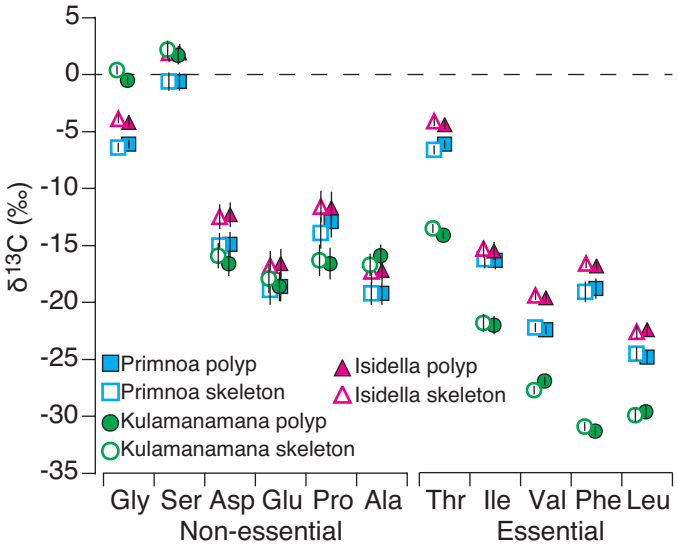
5
0
-5
-10
-15
-20
-25
-30
-35
δ13C (‰)
Primnoa polyp
Primnoa skeleton
Kulamanamana polyp
Kulamanamana skeleton
Isidella polyp
Isidella skeleton
Gly Ser Asp Glu Pro Ala
Non-essential
Thr Ile Val Phe Leu
Essential

Figure 2.

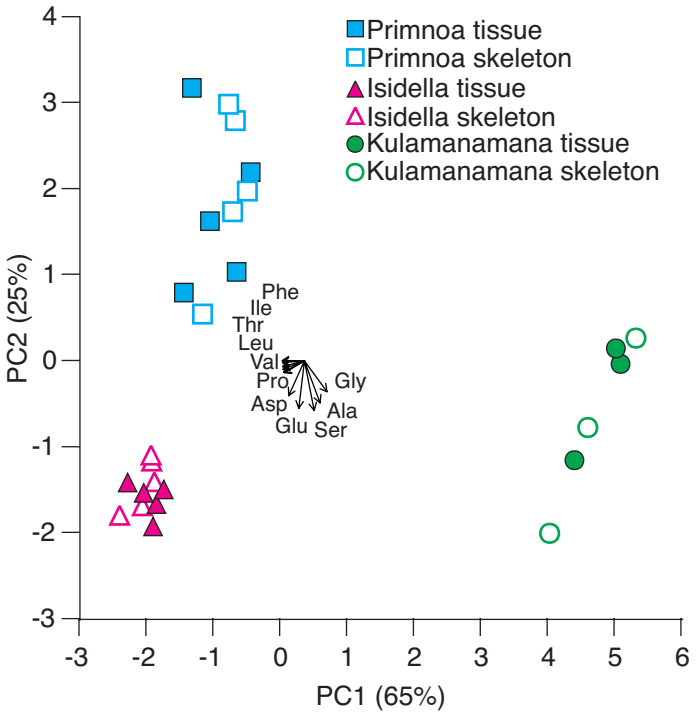
Primnoa tissue
Primnoa skeleton
Isidella tissue
Isidella skeleton
Kulamanamana tissue
Kulamanamana skeleton
Phe
Ile
Thr
Leu
Val
Pro
Asp
Glu
Gly
Ala
Ser
PC2 (25%)
PC1 (65%)
4
3
2
1
0
-1
-2
-3
-3
-2
-1
0
1
2
3
4
5
6

Figure 3.

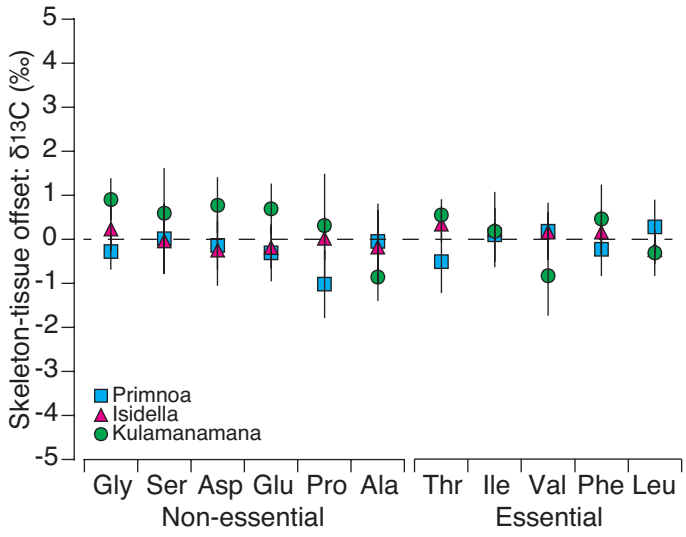
Skeleton-tissue offset: δ13C (‰)
5
4
3
2
1
0
-1
-2
-3
-4
-5
Primnoa
Isidella
Kulamanamana
Gly
Ser
Asp
Glu
Pro
Ala
Thr
Ile
Val
Phe
Leu
Non-essential
Essential

Figure 4.

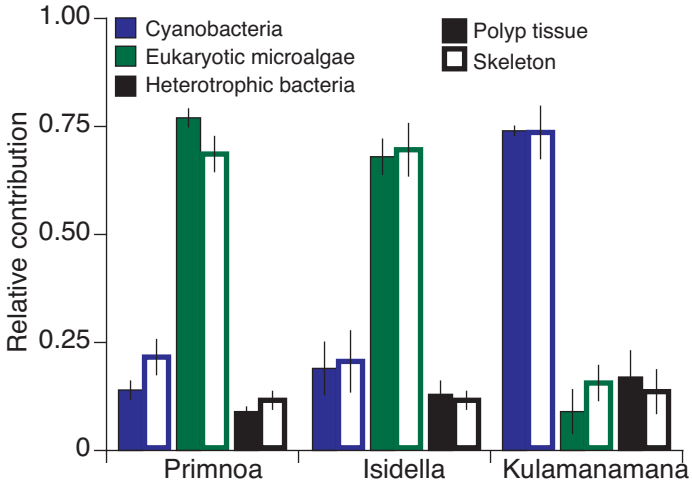
1.00
0.75
0.50
0.25
0
Relative contribution
Cyanobacteria
Eukaryotic microalgae
Heterotrophic bacteria
Polyp tissue
Skeleton
Primnoa
Isidella
Kulamanamana

Figure 5.

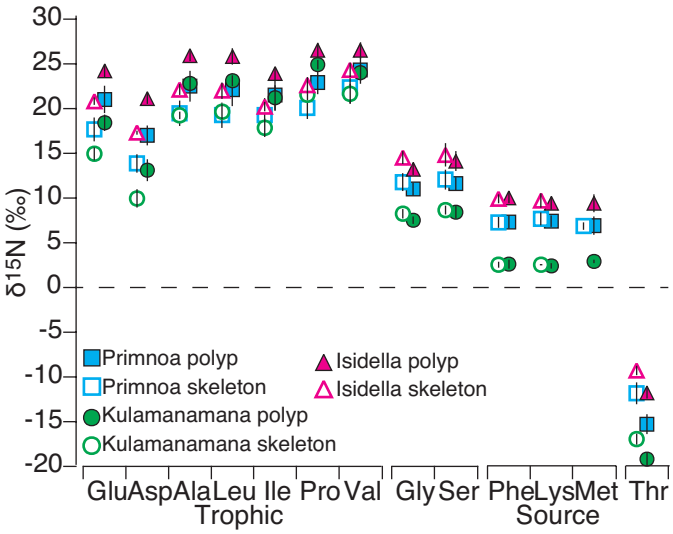
30
25
20
15
10
5
0
-5
-10
-15
-20
δ15N (‰)
Primnoa polyp
Primnoa skeleton
Kulamanamana polyp
Kulamanamana skeleton
Isidella polyp
Isidella skeleton
Glu Asp Ala Leu Ile Pro Val Gly Ser Phe Lys Met Thr
Trophic
Source

Figure 6.

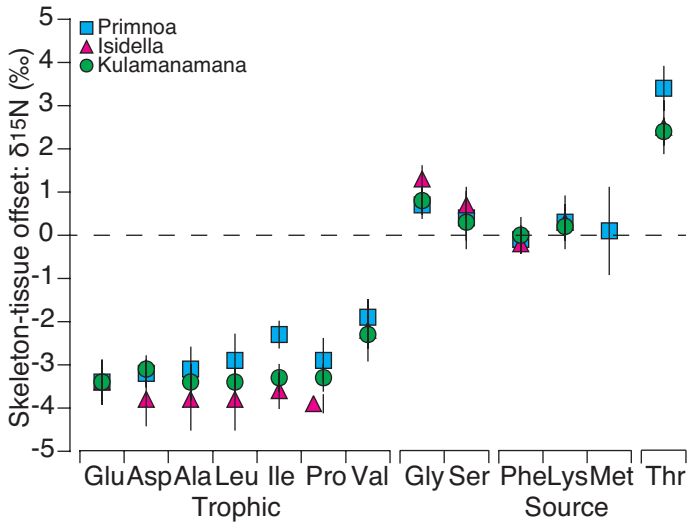

1122

1123 *Figure 7.*

SUPPLEMENTAL MATERIAL

Calibrating amino acid $\delta^{13}C$ and $\delta^{15}N$ offsets between polyp and protein skeleton to develop proteinaceous deep-sea corals as paleoceanographic archives.

Kelton W. McMahon[a,b,c*], Branwen Williams[c], Thomas P. Guilderson[b,e], Danielle S. Glynn[d], and Matthew D. McCarthy[d]

[a]Graduate School of Oceanography, University of Rhode Island, Narragansett, RI 02882 USA

[b]Institute of Marine Sciences, University of California – Santa Cruz, Santa Cruz, CA 95064 USA

[c]W.M. Keck Science Department of Claremont McKenna College, Pitzer College, and Scripps College, Claremont, CA 91711, USA

[d]Ocean Sciences Department, University of California – Santa Cruz, Santa Cruz, CA 95064 USA

[e]Lawrence Livermore National Laboratory, Livermore, California 94550, USA.

*Corresponding Author: K. McMahon (kelton_mcmahon@uri.edu)

Co-authors: B. Williams (bwilliams@kecksci.claremont.edu); T. Guilderson (guilderson1@llnl.gov); D. Glynn (dglynn@ucsc.edu); M. McCarthy (mdmccar@ucsc.edu)

Abbreviations as a footnote

AA: Amino acid; CSI-AA: Compound-specific stable isotopes of amino acids; SIA: Stable isotope analysis; SIAR: Stable Isotope Analysis in R; TP_{CSI-AA}: Trophic position from compound-specific stable isotope of amino acids.

APPENDIX A

Table A.1. Collection information for three genera of proteinaceous deep-sea coral, *Primnoa pacifica* (n = 5) from the Gulf of Alaska (GOA), *Isidella sp.* (n = 5) from the Central California Margin, and *Kulamanamana haumeaae* (n = 3) from the North Pacific Subtropical Gyre (NPSG) (Fig. 1). The dash (-) symbol indicates an unknown depth for GB2, which was collected opportunistically.

Taxa	ID	Region	Depth (m)	Latitude (N)	Longitude (W)
Primnoa	GOA-13-004	GOA	25	58.3	149.5
Primnoa	GOA-13-005	GOA	23	59.5	145.3
Primnoa	GOA-13-011	GOA	191	56.2	135.1
Primnoa	GOA-13-046	GOA	165	56.2	135.1
Primnoa	GOA-GB2	GOA	-	58.9	136.8
Isidella	D620#3	CCM	1224	36.4	122.3
Isidella	D620#4	CCM	1127	36.4	122.3
Isidella	D639#2	CCM	1230	36.4	122.3
Isidella	D641#1	CCM	1247	36.4	122.3
Isidella	D641#2	CCM	1248	36.4	122.3
Kulamanamana	PV588Ger13	NPSG	404	18.7	158.3
Kulamanamana	PV588Ger11	NPSG	394	18.7	158.3
Kulamanamana	PV694Ger14	NPSG	356	23.9	165.4

Primnoa pacifica from the Gulf of Alaska

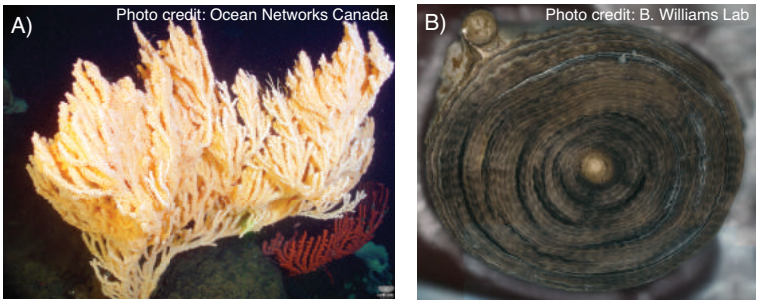

Isidella sp. from the Central California Margin

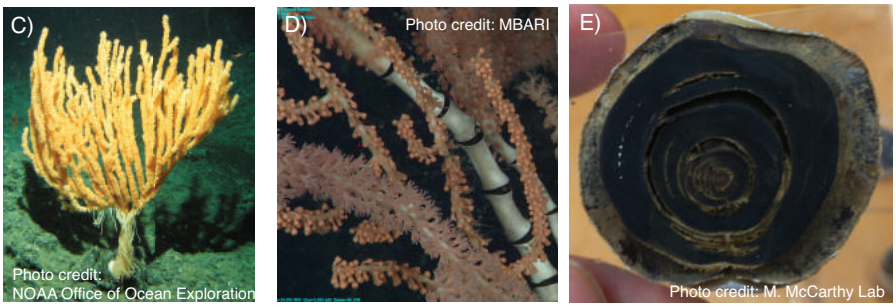

Kulamanamana haumeaae from the North Pacific Subtropical Gyre

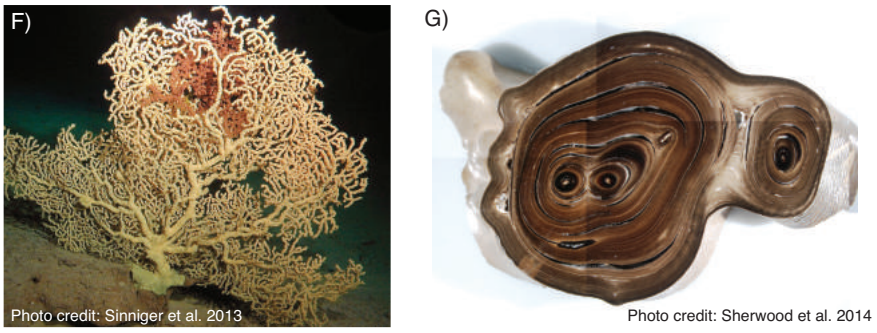

Figure A.1. Deep-sea corals. Photos of deep-sea coral colonies and proteinaceous skeletons for three genera of proteinaceous deep-sea coral, *Primnoa pacifica* from the coastal region of the Gulf of Alaska, *Isidella sp.* from Sur Ridge in the Central California Margin, and *Kulamanamana haumeaae* from the Hawaiian Archipelago in the North Pacific Subtropical Gyre. A) *Primnoa* colony (Photo credit: Ocean Networks Canada), B) *Primnoa* cross-section (B. Williams Lab), C) *Isidella* colony (NOAA Office of Ocean Exploration), D) *Isidella* colony branching pattern (Monterey Bay Aquarium Research Institute), E) *Isidella* proteinaceous skeleton cross-section (M. McCarthy Lab), F) *Kulamanamana* colony (Sinniger et al. 2013), G) *Kulamanama* proteinaceous skeleton cross-section (Sherwood et al. 2014).

APPENDIX B

Much of the recent proxy development work with proteinaceous deep-sea corals has focused on stable isotope analysis (SIA) of total ("bulk") skeletal material, as a proxy for changes in surface ocean conditions (e.g., Heikoop et al. 2002; Sherwood et al. 2005, 2009; Williams et al. 2007; Hill et al. 2014). We conducted bulk $\delta^{13}C$ and $\delta^{15}N$ analyses on all paired polyp tissue and proteinaceous skeleton samples from the three genera of deep-sea corals. For bulk $\delta^{13}C$ analyses of skeleton, a subset of each skeleton sample was individually acid washed in 1 N HCl in glass vials for four hours, rinsed three times in Milli-Q water, and dried over night at 50°C to remove calcium carbonate and isolate the organic fraction of the skeleton. Bulk $\delta^{15}N$ analyses were conducted on non-acidified skeleton samples. Deep-sea coral polyp tissues are very lipid rich (Hamoutene et al. 2008), and therefore a subset of each polyp sample was lipid extracted three times following the conventional methanol/chloroform protocol of Bligh and Dyer (1959) prior to $\delta^{13}C$ analysis. Bulk $\delta^{15}N$ analyses were conducted on non-lipid extracted polyp samples.

Bulk stable carbon ($\delta^{13}C$) and stable nitrogen ($\delta^{15}N$) isotopes were measured on a 0.3 mg aliquot of each sample using a Carlo Erba 1108 elemental analyzer interfaced to a Thermo Finnegan Delta Plus XP isotope ratio mass spectrometer (IRMS) at the Stable Isotope Lab, University of California, Santa Cruz. Raw isotope values were corrected for instrument drift and linearity effects, calibrated against the in house isotopic reference materials of the Stable Isotope Laboratory (http://emerald.ucsc.edu/~silab/), and reported in per mil (‰) relative to Vienna PeeDee Belemnite and air for carbon and nitrogen, respectively. Reproducibility of two lab standards was 0.05‰ and 0.15‰ for carbon and nitrogen isotopes, respectively. Bulk tissue and individual AA stable isotope offsets were calculated as the difference in isotope value ($\delta^{13}C$ or

73 $\delta^{15}N$) between paired polyp and skeleton samples for each specimen within each genus of deep-
74 sea coral.

75 Carbon isotopes have long been used to infer sources of primary producers contributing
76 to food web architecture (Wada et al. 1991; Boecklen et al. 2011). Bulk $\delta^{13}C$ were generally
77 more positive in *Primnoa* from the Gulf of Alaska and *Isidella* from the Sur Ridge than
78 *Kulamanamana* from the NPSG (Table B.1). However, interpreting past changes in primary
79 producer composition from these bulk carbon isotope values is challenging (Schiff et al. 2014;
80 McMahon et al. 2015a). For example, we found large differences in the bulk $\delta^{13}C$ values (mean
81 offset = 3.5 ± 0.5‰ averaged across all three species) and C/N ratio (mean offset = 1.9 ± 0.7)
82 between lipid-intact coral polyp tissue and recently deposited protein skeleton within single
83 colonies. These offsets were far greater than the differences in $\delta^{13}C$ value (1-2‰ for a given
84 tissue) among different genera of corals collected from vastly different oceanographic regimes
85 (Table B.1). This intra-colony offset likely reflects differences in macromolecular tissue
86 composition (lipid, AA, carbonate) rather than environmental drivers. Once lipids were removed
87 from the polyp tissue, there was only a small difference in bulk $\delta^{13}C$ value (mean offset = -0.4 ±
88 0.1‰ averaged across all three species) and C/N ratio (mean offset = 0.2 ± 0.3) between
89 proteinaceous skeleton and polyp tissue for all species. However, even after bulk lipid extraction
90 of polyp tissue and decalcification of skeleton material, the remaining confounding influences of
91 primary producer source and trophic dynamics make interpreting bulk $\delta^{13}C$ variability among
92 specimens very challenging.

93 Stable nitrogen isotopes of consumers reflect both the source of nitrogen at the base of
94 the food web and the number of trophic transfers between that base and the consumer (Boecklen
95 et al. 2011). While these factors may explain the significant differences in bulk tissue $\delta^{15}N$

values among the proteinaceous deep-sea coral species (~6‰) in our study (Table B.1), we also found a moderate offset in bulk $\delta^{15}N$ value (1.9 ± 0.7‰ across all three species) between polyp tissue and proteinaceous skeleton within colonies (Table B.1). As with bulk $\delta^{13}C$ differences discussed above, such offsets between tissue types of the same individuals are likely due primarily to biochemical composition: i.e., the larger diversity of nitrogenous organic molecules in coral polyp as compared with its skeleton, as well as the highly selected AA composition of the specialized gorgonin structural protein found in proteinaceous skeleton (Goodfriend et al. 1997; Ehrlich 2010). Bulk $\delta^{15}N$ isotope data therefore can be even more challenging to interpret than bulk $\delta^{13}C$ data, given the potential differences in tissue composition within and among species, as well as the much larger influence of $\delta^{15}N_{baseline}$ and trophic position.

Table B.1.

Bulk $\delta^{13}C$ (‰) in proteinaceous skeleton (acidified), polyp tissue with and without lipids intact, and the offset in $\delta^{13}C$ value between skeleton and polyp from three genera of proteinaceous deep-sea coral: *Primnoa pacifica*, *Isidella sp.*, and *Kulamanamana haumeaae*. Bulk $\delta^{15}N$ (‰) in proteinaceous skeleton (non-acidified), polyp tissue (lipids intact), and the offset in $\delta^{15}N$ value between skeleton and polyp from the same corals. C/N ratios of coral skeleton, and polyps and without lipids intact.

	$\delta^{13}C$					**$\delta^{15}N$**		
	Skeleton	Polyp w/ lipids	Polyp w/o lipids	Offset w/ lipids	Offset w/o lipids	Skeleton	Polyp w/ lipids	Offset
Primnoa_GOA_13_004	-17.3	-19.5	-16.3	2.2	-1.0	11.8	15.4	-3.6
Primnoa_GOA_13_005	-15.4	-18.5	-14.9	3.1	-0.5	10.9	12.6	-1.7
Primnoa_GOA_13_011	-15.3	-20.3	-15.4	5.0	0.1	11.2	13.3	-2.1
Primnoa_GOA_13_046	-14.1	-20.3	-14.7	6.2	0.6	10.8	13.6	-2.7
Primnoa_GB2	-15.8	-19.7	-15.3	3.9	-0.5	11.1	14.1	-3.0
Isidella_D620#3	-15.1	-17.9	-14.6	2.8	-0.5	14.0	14.8	-0.8
Isidella _D620#4	-16.1	-18.3	-15.3	2.2	-0.8	15.2	16.4	-1.2
Isidella _D639#2	-15.9	-18.8	-15.4	2.9	-0.5	15.1	16.3	-1.2
Isidella _D641#1	-15.2	-18.0	-14.6	2.8	-0.5	14.4	16.2	-1.8
Isidella _D641#2	-15.1	-19.7	-15.5	4.6	0.4	15.3	16.3	-1.0
Kulamanamana_PV588Ger13	-16.9	-20.5	-16.5	3.6	-0.4	8.1	10.5	-2.4
Kulamanamana_PV588Ger11	-16.9	-20.4	-16.4	3.5	-0.5	8.6	9.9	-1.4
Kulamanamana_PV694Ger14	-17.0	-20.3	-16.4	3.2	-0.6	8.2	10.4	-2.1

127 *Table B.1 cont.*

	C/N Ratio		
	Skeleton	Polyp w/Lipids	Polyps w/o lipids
Primnoa_GOA_13_004	3.1	5.3	3.2
Primnoa_GOA_13_005	3.3	6.8	3.4
Primnoa_GOA_13_011	3.4	4.5	3.2
Primnoa_GOA_13_046	2.9	4.2	3.4
Primnoa_GB2	2.8	4.8	3.5
Isidella_D620#3	2.6	4.5	3.2
Isidella _D620#4	2.7	4.7	2.9
Isidella _D639#2	3.3	4.8	3.2
Isidella _D641#1	2.6	4.8	2.8
Isidella _D641#2	2.7	5.1	3.3
Kulamanamana_PV588Ger13	3.2	4.4	2.8
Kulamanamana_PV588Ger11	2.8	4.3	2.8
Kulamanamana_PV694Ger14	2.8	4.1	2.8

APPENDIX C

We used principal component analysis to visualize multivariate patterns in the $\delta^{13}C$ values of individual AAs (Ala, Asp, Gly, Glu, Ile, Leu, Phe, Pro, Ser, Thr, Val; Table C.5) in polyp tissue and skeleton of the three deep-sea coral genera (Fig. 3). The first two principal components explained 90.3% of the total variation in the model (PC1 = 64.8%, PC2 = 25.5%) (Table C.5). The skeleton and polyp tissue AA $\delta^{13}C$ values from a single genus always clustered together in multivariate space, and all three corals were well separated in multivariate space (Fig. 3). Along the first principal component, the essential AAs Ile (-0.37), Phe (-0.37), Thr (-0.37), Leu (0.36), and Val (-0.35) were the most powerful separators (Table B.1). Along the second principal component, the non-essential AAs Ser (-0.53), Glu (-0.51), Ala (-0.45), Asp (-0.36), and Gly (-0.32) showed the greatest separation power (Table C.5).

We used an AA isotope fingerprinting approach to examine the composition of primary producers fueling export production to deep-sea corals in each of the three study regions: Gulf of Alaska (*Primnoa*), Central California Margin (*Isidella*), and NPSG (*Kulamanamana*) (sensu McMahon et al. 2015a). We characterized unique AA isotope fingerprints for three source end-members, eukaryotic microalgae, prokaryotic cyanobacteria, and heterotrophic bacteria, that are key contributors to the plankton communities of the North Pacific Ocean (Chavez et al. 1991; Odate 1996; Karl et al. 2001). The source end-members were based on a subset of molecular-isotopic training data sets from Lehman (2009) (culture conditions presented in McCarthy et al. 2013) and Larsen et al. (2009; 2013) (Table C.6).

We focused our fingerprinting analyses on five essential AAs (threonine, valine, isoleucine, phenylalanine, and leucine). The essential AA $\delta^{13}C$ values represent the sum of the isotopic fractionations associated with individual biosynthetic pathways and associated branch

151 points for each EAA (Hayes 2001; Scott et al. 2006), generating AA $\delta^{13}C$ fingerprints of the
152 primary producer sources that made those AAs (Larsen et al. 2009; 2013). In order to compare
153 the essential AA $\delta^{13}C$ fingerprints of our three source end-member groups and corals across
154 different regions and time periods, we examined essential AA $\delta^{13}C$ values normalized to the
155 mean of all five essential AAs for each sample. To do this, we subtracted the mean of all five
156 essential AA $\delta^{13}C$ values from each individual essential AA $\delta^{13}C$ value for each sample (senus
157 Larsen et al. 2015). All three source end-members have very distinct essential AA $\delta^{13}C$
158 fingerprints, with within-group variability far smaller than among group variability despite
159 samples coming from laboratory and field collections across a range of environmental gradients.
160 There is strong experimental and field-based evidence that primary producer essential
161 AA $\delta^{13}C$ fingerprints are faithful and robust across large environmental gradients in growing
162 conditions and carbon sources that can affect bulk $\delta^{13}C$ values (Larsen et al. 2013, 2015). This is
163 because the underlying biochemical mechanisms generating unique internally normalized
164 essential AA $\delta^{13}C$ fingerprints are driven by major evolutionary diversity in the central synthesis
165 and metabolism of AAs. For example, Larsen et al. (2013) examined the extent to which
166 normalized essential AA $\delta^{13}C$ fingerprints were affected by environmental conditions by looking
167 at seagrass (*Posidonia oceanica*) and giant kelp communities (*Macrocystis pyrifera*) across a
168 variety of oceanographic and growth conditions (see Larsen et al. 2013 Table S1 for details). For
169 both species, the range in bulk $\delta^{13}C$ values was five- to ten-times greater (2.6‰ and 5.2‰,
170 respectively) than it was for normalized essential AA $\delta^{13}C$ values (0.4‰ to 0.6‰, respectively).
171 By normalizing the individual essential AA $\delta^{13}C$ values to the mean, Larsen et al. (2013) showed
172 that natural variability in $\delta^{13}C$ values of individual amino acids is effectively removed, creating
173 diagnostic fingerprints that were independent of environmental conditions.

Larsen et al. (2015) also conducted the first directly controlled physiological studies of normalized essential AA $\delta^{13}C$ fingerprint fidelity using a laboratory-cultured marine diatom, *Thalassiosira weissflogii*, grown under a wide range of conditions: light, salinity, temperature, and pH. This study showed that normalized essential AA $\delta^{13}C$ values remained essentially unmodified despite very large changes in bulk and raw amino acid $\delta^{13}C$ values (>10‰), molar percent abundances of individual amino acids, and total cellular carbon to nitrogen ratios. Together, Larsen et al. (2013, 2015) provide strong evidence that normalized essential AA $\delta^{13}C$ fingerprints are diagnostic of the primary producer source rather than the myriad factors affecting bulk $\delta^{13}C$ values such as carbon availability, growth conditions, and oceanographic conditions. Results from Schiff et al. (2014) also support this conclusion for deep-sea corals by showing excellent agreement between the normalized essential AA $\delta^{13}C$ fingerprints of deep-sea bamboo coral, *Isidella sp.*, from Monterey Canyon, California and field-collected eukaryotic microalgae from the California coast (Vokhshoori et al. 2014). Similarly, McMahon et al. (2016) showed that while the essential amino acid $\delta^{13}C$ values of lab cultures of zooxanthellate dinoflagellates were significantly different than the essential amino acid $\delta^{13}C$ values of zooxanthellate dinoflagellates in wild corals, when the essential amino acid $\delta^{13}C$ were normalized to the mean of all essential amino acids in each individual sample, the cultured and wild samples became indistinguishable in multivariate PCA space. As such, we are confident that the normalized essential AA $\delta^{13}C$ fingerprints of laboratory-cultured and field-collected source end-members are robust, faithful proxies of the identity of major carbon sources for deep-sea corals, regardless of the exact location and growing conditions of the end-members.

Table C.1. Mean individual amino acid $\delta^{13}C$ values (‰ ± SD) in proteinaceous skeleton from three genera of proteinaceous deep-sea coral: *Primnoa pacifica*, *Isidella sp.*, and *Kulamanamana haumeaae*. SD reflects the analytical variability for each amino acid calculated from triplicate analyses of each derivatized sample.

	Ala	Asp	Glu	Gly	Ile	Leu	Phe	Pro
Primnoa_GOA_13_004	-18.3 ± 0.2	-14.0 ± 0.2	-19.1 ± 0.1	-6.8 ± 0.1	-15.9 ± 0.2	-24.8 ± 0.2	-19.2 ± 0.5	-14.0 ± 0.6
Primnoa_GOA_13_005	-18.4 ± 0.6	-13.7 ± 0.5	-17.1 ± 0.3	-6.7 ± 0.5	-16.1 ± 0.6	-24.3 ± 0.8	-18.7 ± 0.1	-13.6 ± 0.5
Primnoa_GOA_13_011	-19.9 ± 0.5	-15.9 ± 0.7	-19.0 ± 0.5	-6.4 ± 0.1	-16.4 ± 0.3	-25.0 ± 0.2	-19.5 ± 0.4	-13.6 ± 0.2
Primnoa_GOA_13_046	-19.9 ± 0.4	-15.3 ± 0.1	-19.1 ± 0.4	-6.8 ± 0.2	-16.1 ± 0.2	-24.6 ± 0.2	-18.4 ± 0.1	-15.6 ± 0.2
Primnoa_GB2	-19.7 ± 0.2	-16.2 ± 0.4	-20.2 ± 0.4	-5.3 ± 0.6	-16.3 ± 0.7	-24.0 ± 0.5	-18.4 ± 0.5	-12.5 ± 0.7
Isidella_D620#3	-17.8 ± 0.6	-12.8 ± 0.6	-16.9 ± 0.6	-3.8 ± 0.4	-15.6 ± 0.1	-23.4 ± 0.2	-17.7 ± 0.1	-12.5 ± 0.5
Isidella _D620#4	-16.9 ± 0.7	-12.6 ± 0.2	-17.3 ± 0.2	-3.7 ± 0.5	-16.1 ± 0.6	-22.7 ± 0.2	-16.8 ± 0.2	-11.0 ± 0.2
Isidella _D639#2	-18.0 ± 0.4	-12.4 ± 0.5	-16.5 ± 0.2	-3.7 ± 0.2	-15.2 ± 0.1	-21.8 ± 0.5	-16.3 ± 0.5	-12.1 ± 0.7
Isidella _D641#1	-16.9 ± 0.4	-13.7 ± 0.5	-17.1 ± 0.5	-4.4 ± 0.2	-14.5 ± 0.2	-23.7 ± 0.6	-16.4 ± 0.1	-12.2 ± 0.5
Isidella _D641#2	-17.6 ± 0.1	-11.7 ± 0.6	-16.8 ± 0.4	-4.6 ± 0.3	-15.1 ± 0.2	-22.0 ± 0.1	-16.4 ± 0.6	-11.0 ± 0.2
Kulamanamana_PV588Ger13	-16.4 ± 0.4	-16.2 ± 0.1	-18.3 ± 0.1	0.5 ± 0.6	-22.0 ± 0.1	-29.6 ± 0.3	-30.3 ± 0.1	-16.0 ± 0.3
Kulamanamana_PV588Ger11	-16.6 ± 0.1	-17.2 ± 0.6	-19.2 ± 0.1	-0.2 ± 0.1	-22.8 ± 0.4	-29.8 ± 0.4	-31.3 ± 0.3	-16.9 ± 0.6
Kulamanamana_PV694Ger14	-17.2 ± 0.1	-14.1 ± 0.3	-16.2 ± 0.2	0.7 ± 0.2	-20.8 ± 0.6	-30.2 ± 0.0	-31.1 ± 0.5	-16.0 ± 0.5

Table C.1 cont.

	Ser	Thr	Val
Primnoa_GOA_13_004	-0.8 ± 0.4	-6.0 ± 0.1	-23.0 ± 0.3
Primnoa_GOA_13_005	-0.3 ± 0.2	-6.1 ± 0.6	-22.2 ± 0.1
Primnoa_GOA_13_011	0.4 ± 0.2	-7.6 ± 0.2	-21.9 ± 0.6
Primnoa_GOA_13_046	-1.3 ± 0.1	-6.9 ± 0.2	-21.8 ± 0.5
Primnoa_GB2	-1.3 ± 0.4	-6.6 ± 0.2	-22.1 ± 0.4
Isidella_D620#3	1.5 ± 0.3	-3.5 ± 0.4	-19.6 ± 0.4
Isidella _D620#4	1.5 ± 0.1	-4.4 ± 0.2	-19.7 ± 0.5
Isidella _D639#2	2.3 ± 0.1	-4.0 ± 0.1	-20.7 ± 0.1
Isidella _D641#1	1.3 ± 0.6	-5.2 ± 0.5	-17.2 ± 0.3
Isidella _D641#2	2.3 ± 0.8	-3.8 ± 0.6	-20.5 ± 0.5
Kulamanamana_PV588Ger13	2.3 ± 0.1	-12.6 ± 0.5	-27.6 ± 0.1
Kulamanamana_PV588Ger11	1.6 ± 0.1	-14.8 ± 0.4	-28.1 ± 0.4
Kulamanamana_PV694Ger14	2.8 ± 0.2	-13.2 ± 0.6	-27.5 ± 0.6

Table C.2. Mean individual amino acid $\delta^{13}C$ values (‰ ± SD) in polyp tissue from three genera of proteinaceous deep-sea coral: *Primnoa pacifica*, *Isidella sp.*, and *Kulamanamana haumeaae*. SD reflects the analytical variability for each amino acid calculated from triplicate analyses of each derivatized sample.

	Ala	Asp	Glu	Gly	Ile	Leu	Phe	Pro
Primnoa_GOA_13_004	-18.4 ± 0.2	-14.6 ± 0.5	-19.4 ± 0.5	-6.0 ± 0.1	-15.3 ± 0.2	-24.0 ± 0.6	-18.3 ± 0.6	-12.6 ± 0.7
Primnoa_GOA_13_005	-18.7 ± 0.2	-13.5 ± 0.6	-17.0 ± 0.2	-6.2 ± 0.1	-15.8 ± 0.5	-24.8 ± 0.3	-19.1 ± 0.2	-13.0 ± 0.5
Primnoa_GOA_13_011	-18.6 ± 0.2	-14.9 ± 0.6	-17.8 ± 0.6	-6.3 ± 0.2	-16.5 ± 0.2	-25.4 ± 0.2	-19.9 ± 0.7	-13.6 ± 0.6
Primnoa_GOA_13_046	-19.5 ± 0.5	-15.3 ± 0.4	-19.3 ± 0.7	-6.5 ± 0.1	-17.1 ± 0.1	-25.0 ± 0.4	-18.0 ± 0.4	-14.4 ± 0.5
Primnoa_GB2	-20.6 ± 0.2	-16.2 ± 0.1	-19.6 ± 0.5	-5.6 ± 0.2	-16.6 ± 0.5	-24.8 ± 0.2	-18.0 ± 0.2	-10.8 ± 0.6
Isidella_D620#3	-17.1 ± 0.1	-12.5 ± 0.6	-16.7 ± 0.2	-3.9 ± 0.5	-14.6 ± 0.4	-23.0 ± 0.3	-17.3 ± 0.1	-11.9 ± 0.1
Isidella _D620#4	-17.7 ± 0.2	-11.9 ± 0.5	-16.6 ± 0.6	-3.5 ± 0.1	-15.9 ± 0.5	-22.9 ± 0.4	-16.9 ± 0.2	-11.3 ± 0.4
Isidella _D639#2	-16.8 ± 0.4	-13.1 ± 0.6	-17.0 ± 0.6	-4.7 ± 0.6	-15.7 ± 0.4	-21.6 ± 0.5	-17.2 ± 0.1	-12.7 ± 0.1
Isidella _D641#1	-17.4 ± 0.3	-12.4 ± 0.5	-16.7 ± 0.1	-4.6 ± 0.4	-15.4 ± 0.6	-23.3 ± 0.2	-16.2 ± 0.6	-12.0 ± 0.1
Isidella _D641#2	-17.3 ± 0.5	-12.0 ± 0.2	-16.7 ± 0.4	-4.7 ± 0.5	-16.0 ± 0.2	-21.5 ± 0.0	-16.7 ± 0.5	-10.9 ± 0.7
Kulamanamana_PV588Ger13	-15.6 ± 0.1	-17.7 ± 0.1	-19.1 ± 0.1	-0.4 ± 0.7	-22.3 ± 0.4	-28.8 ± 0.2	-30.9 ± 0.4	-17.4 ± 0.5
Kulamanamana_PV588Ger11	-16.2 ± 0.8	-17.5 ± 0.4	-19.3 ± 0.3	-1.5 ± 0.4	-22.8 ± 0.3	-29.5 ± 0.5	-32.4 ± 0.8	-16.0 ± 0.2
Kulamanamana_PV694Ger14	-15.8 ± 0.1	-14.7 ± 0.1	-17.4 ± 0.6	0.3 ± 0.2	-20.9 ± 0.1	-30.4 ± 0.4	-30.7 ± 0.6	-16.4 ± 0.2

224 Table C.2 cont.

	Ser	Thr	Val
Primnoa_GOA_13_004	-0.4 ± 0.6	-6.2 ± 0.3	-22.4 ± 0.5
Primnoa_GOA_13_005	-1.0 ± 0.1	-6.2 ± 0.2	-22.0 ± 0.3
Primnoa_GOA_13_011	0.0 ± 0.5	-6.2 ± 0.4	-22.7 ± 0.1
Primnoa_GOA_13_046	-0.2 ± 0.2	-6.5 ± 0.1	-22.7 ± 0.2
Primnoa_GB2	-1.7 ± 0.6	-5.6 ± 0.7	-22.1 ± 0.6
Isidella_D620#3	1.8 ± 0.2	-3.7 ± 0.3	-19.9 ± 0.1
Isidella _D620#4	2.2 ± 0.1	-5.1 ± 0.2	-19.6 ± 0.2
Isidella _D639#2	2.0 ± 0.3	-3.7 ± 0.5	-20.3 ± 0.1
Isidella _D641#1	1.8 ± 0.6	-5.9 ± 0.1	-17.9 ± 0.4
Isidella _D641#2	1.3 ± 0.2	-4.1 ± 0.2	-20.7 ± 0.4
Kulamanamana_PV588Ger13	1.7 ± 0.1	-12.9 ± 0.4	-27.3 ± 0.1
Kulamanamana_PV588Ger11	2.1 ± 0.6	-15.2 ± 0.5	-26.2 ± 0.2
Kulamanamana_PV694Ger14	1.2 ± 0.5	-14.1 ± 0.3	-27.1 ± 0.1

225

226

227

228

229

230

231

232

233 Table C.3. Mean individual amino acid $\delta^{15}N$ values (‰ ± SD) in proteinaceous skeleton from three genera of proteinaceous deep-sea
234 coral: *Primnoa pacifica*, *Isidella sp.*, and *Kulamanamana haumeaae*. SD reflects the analytical variability for each amino acid
235 calculated from triplicate analyses of each derivatized sample. na = not analyzed

	Ala	Asp	Glu	Gly	Ile	Leu	Lys	Met
Primnoa_GOA_13_004	21.1 ± 0.3	14.8 ± 0.1	18.9 ± 0.6	11.9 ± 0.2	22.3 ± 0.1	21.1 ± 0.2	8.2 ± 0.4	7.0 ± 0.3
Primnoa_GOA_13_005	18.6 ± 0.1	12.7 ± 0.5	16.7 ± 0.2	10.7 ± 0.8	18.1 ± 0.2	17.6 ± 0.5	7.2 ± 0.1	6.4 ± 0.1
Primnoa_GOA_13_011	19.4 ± 0.4	13.1± 0.6	16.9 ± 0.6	12.2 ± 0.1	18.0 ± 0.2	19.0 ± 0.1	7.5 ± 0.0	6.6 ± 0.2
Primnoa_GOA_13_046	20.2 ± 0.5	13.8 ± 0.5	18.8 ± 0.1	11.0 ± 0.1	19.3 ± 0.6	19.5 ± 0.1	8.2 ± 0.5	8. 0± 0.2
Primnoa_GB2	17.8 ± 0.1	14.5 ± 0.6	16.6 ± 0.2	12.8 ± 0.6	18.4 ± 0.5	18.9 ± 0.4	7.0 ± 0.4	7.2 ± 0.5
Isidella_D620#3	22.3 ± 0.1	17.5 ± 0.2	21.2 ± 0.1	14.4 ± 0.4	20.6 ± 0.2	22.3 ± 0.2	9.1 ± 0.4	na
Isidella _D620#4	22.8 ± 0.1	17.6 ± 0.5	20.8 ± 0.6	14.7± 0.1	21.0 ± 0.2	22.2 ± 0.7	9.6 ± 0.0	na
Isidella _D639#2	22.6 ± 0.7	17.5 ± 0.3	21.2 ± 0.2	14.2 ± 0.6	20.2 ± 0.4	23.2 ± 0.5	9.6 ± 0.6	na
Isidella _D641#1	21.4 ± 0.6	17.5 ± 0.6	20.7 ± 0.5	15.8 ± 0.4	19.9 ± 0.5	20.9 ± 0.2	10.7 ± 0.2	na
Isidella _D641#2	22.2 ± 0.1	17.3 ± 0.2	21.3 ± 0.3	14.6 ± 0.4	20.4 ± 0.5	22.6 ± 0.2	10.7 ± 0.4	na
Kulamanamana_PV588Ger13	19.6 ± 0.2	11.0 ± 0.4	15.5 ± 0.5	8.3 ± 0.4	18.4 ± 0.6	19.8 ± 0.1	2.6 ± 0.2	na
Kulamanamana_PV588Ger11	19.3 ± 0.4	9.9 ± 0.3	15.0 ± 0.2	8.0 ± 0.1	18.5 ± 0.1	20.3 ± 0.3	2.5 ± 0.3	na
Kulamanamana_PV694Ger14	19.1 ± 0.3	9.1 ± 0.6	14.3 ± 0.4	8.7 ± 0.1	16.8 ± 0.1	19.0 ± 0.1	2.6 ± 0.6	na

236
237
238
239
240
241

Table C.3 cont.

	Phe	Pro	Ser	Thr	Val
Primnoa_GOA_13_004	8.0 ± 0.2	21.3 ± 0.4	11.8 ± 0.2	-12.8 ± 0.5	24.7 ± 0.3
Primnoa_GOA_13_005	6.9 ± 0.5	18.2 ± 0.5	11.4 ± 0.6	-11.4 ± 0.2	20.2 ± 0.1
Primnoa_GOA_13_011	6.9 ± 0.1	19.5 ± 0.5	10.8 ± 0.6	-11.7± 0.6	21.5 ± 0.4
Primnoa_GOA_13_046	6.8 ± 0.2	20.6 ± 0.3	12.4 ± 0.5	-13.2 ± 0.1	23.0 ± 0.5
Primnoa_GB2	7.4 ± 0.6	20.1 ± 0.6	13.5 ± 0.8	-10.6 ± 0.1	22.2 ± 0.1
Isidella_D620#3	9.7 ± 0.3	22.0 ± 0.2	13.2 ± 0.5	-8.9 ± 0.2	24.5 ± 0.1
Isidella _D620#4	9.4 ± 0.2	22.9 ± 0.8	14.7 ± 0.0	-9.4 ± 0.1	24.0 ± 0.1
Isidella _D639#2	10.4 ± 0.6	23.3 ± 0.8	15.4 ± 0.1	-8.6 ± 0.4	24.4 ± 0.4
Isidella _D641#1	10.3 ± 0.4	21.9 ± 0.6	16.6 ± 0.2	-9.2 ± 0.3	24.1 ± 0.2
Isidella _D641#2	10.4 ± 0.6	23.6 ± 0.8	14.9 ± 0.1	-9.5 ± 0.2	25.7 ± 0.2
Kulamanamana_PV588Ger13	2.6 ± 0.8	21.5 ± 0.2	8.6 ± 0.5	-16.4 ± 0.5	22.3 ± 0.6
Kulamanamana_PV588Ger11	2.8 ± 0.5	22.2 ± 0.5	8.4 ± 0.4	-16.9 ± 0.6	22.3 ± 0.1
Kulamanamana_PV694Ger14	2.3 ± 0.4	21.2 ± 0.2	9.2 ± 0.3	-17.3 ± 0.2	20.6 ± 0.2

Table C.4. Mean individual amino acid $\delta^{15}N$ values (‰ ± SD) in polyp tissue from three genera of proteinaceous deep-sea coral: *Primnoa pacifica*, *Isidella sp.*, and *Kulamanamana haumeaae*. SD reflects the analytical variability for each amino acid calculated from triplicate analyses of each derivatized sample.

Tissue	Ala	Asp	Glu	Gly	Ile	Leu	Lys	Met
Primnoa_GOA_13_004	24.7 ± 0.1	18.5 ± 0.7	22.9 ± 0.2	11.3 ± 0.1	24.2 ± 0.5	24.9 ± 0.1	7.3 ± 0.6	6.2 ± 0.2
Primnoa_GOA_13_005	21.2 ± 0.2	15.8 ± 0.2	19.5 ± 0.2	10.1 ± 0.5	20.1 ± 0.1	20.6 ± 0.4	6.6 ± 0.5	6.0 ± 0.4
Primnoa_GOA_13_011	22.1 ± 0.5	16.5 ± 0.1	20.6 ± 0.6	11.4 ± 0.2	20.8 ± 0.4	21.1 ± 0.6	7.5 ± 0.5	7.2 ± 0.1
Primnoa_GOA_13_046	23.7 ± 0.6	16.8 ± 0.2	21.9 ± 0.2	10.6 ± 0.1	21.5 ± 0.3	22.4 ± 0.2	7.8 ± 0.6	8.3 ± 0.4
Primnoa_GB2	20.9 ± 0.2	17.3 ± 0.7	20.0 ± 0.4	11.6 ± 0.4	20.9 ± 0.7	21.8 ± 0.1	7.6 ± 0.4	6.8 ± 0.2
Isidella_D620#3	26.6 ± 0.6	21.4 ± 0.4	25.1 ± 0.1	13.2 ± 0.3	24.0 ± 0.2	25.7 ± 0.1	8.8 ± 0.1	8.2 ± 0.4
Isidella _D620#4	26.6 ± 0.5	20.6 ± 0.5	23.6 ± 0.5	13.0 ± 0.2	24.8 ± 0.5	25.9 ± 0.1	9.2 ± 0.6	9.5 ± 0.2
Isidella _D639#2	25.7 ± 0.4	21.1 ± 0.4	24.1 ± 0.6	13.2 ± 0.3	23.3 ± 0.3	26.1 ± 0.1	9.9 ± 0.3	10.1 ± 0.5
Isidella _D641#1	25.5 ± 0.4	21.6 ± 0.1	24.1 ± 0.1	14.2 ± 0.2	23.7 ± 0.7	25.1± 0.2	10.1 ± 0.2	10.3 ± 0.6
Isidella _D641#2	26.7 ± 0.4	21.8 ± 0.5	25.0 ± 0.2	13.4 ± 0.2	24.5 ± 0.6	27.2 ± 0.3	10.2 ± 0.2	10.1 ± 0.2
Kulamanamana_PV588Ger13	23.3 ± 0.4	14.3 ± 0.1	19.0 ± 0.2	7.7 ± 0.2	22.0 ± 0.1	23.9 ± 0.6	2.1 ± 0.3	2.9 ± 0.1
Kulamanamana_PV588Ger11	23.0 ± 0.2	12.7 ± 0.2	18.6 ± 0.1	7.2 ± 0.2	21.9 ± 0.1	23.6 ± 0.1	2.4 ± 0.2	2.9 ± 0.6
Kulamanamana_PV694Ger14	22.0 ± 0.5	12.2 ± 0.5	17.5 ± 0.3	7.6 ± 0.5	19.8 ± 0.4	22.6 ± 0.2	2.5 ± 0.1	2.7 ± 0.5

Table C.4 cont.

	Phe	Pro	Ser	Thr	Val
Primnoa_GOA_13_004	7.8 ± 0.3	24.4 ± 0.2	11.9 ± 0.1	-16.4 ± 0.6	26.5 ± 0.6
Primnoa_GOA_13_005	6.6 ± 0.1	21.2 ± 0.7	10.7 ± 0.3	-14.2 ± 0.0	22.8 ± 0.3
Primnoa_GOA_13_011	7.3 ± 0.6	23.1 ± 0.2	11.3 ± 0.7	-15.4 ± 0.1	23.6 ± 0.1
Primnoa_GOA_13_046	6.8 ± 0.6	23.2 ± 0.1	11.7 ± 0.6	-16.2 ± 0.2	24.4 ± 0.1
Primnoa_GB2	7.9 ± 0.1	22.6 ± 0.1	12.4 ± 0.5	-14.5 ± 0.4	24.0 ± 0.1
Isidella_D620#3	9.8 ± 0.0	26.2 ± 0.5	13.0 ± 0.6	-11.6 ± 0.6	27.3 ± 0.2
Isidella _D620#4	9.5 ± 0.2	26.9 ± 0.5	13.6 ± 0.7	-12.0 ± 0.3	27.1 ± 0.4
Isidella _D639#2	10.7 ± 0.5	26.9 ± 0.5	14.8 ± 0.5	-11.7 ± 0.5	26.1 ± 0.4
Isidella _D641#1	10.3 ± 0.5	25.9 ± 0.6	15.6 ± 0.4	-10.8 ± 0.5	25.7 ± 0.4
Isidella _D641#2	10.8 ± 0.7	27.6 ± 0.3	14.3 ± 0.1	-12.2 ± 0.2	27.5 ± 0.2
Kulamanamana_PV588Ger13	2.1 ± 0.4	25.1 ± 0.1	7.8 ± 0.2	-18.4 ± 0.2	24.3 ± 0.3
Kulamanamana_PV588Ger11	2.8 ± 0.5	25.3 ± 0.7	8.4 ± 0.1	-19.4 ± 0.1	24.5 ± 0.2
Kulamanamana_PV694Ger14	2.7 ± 0.1	24.4 ± 0.2	9.1 ± 0.6	-19.8 ± 0.6	23.1 ± 0.1

Table C.5. Eigenvectors and variance explained (%) for the eleven principal components (PC) in the principal component analysis (Fig. 3) of eleven individual amino acid $\delta^{13}C$ values from polyp tissues and proteinaceous skeleton of three species of deep-sea corals: *Primnoa pacifica* (n = 5 individual colonies) from the Gulf of Alaska, *Isidella sp.* (n = 5 individual colonies) from the Central California Margin, and *Kulamanamana haumeaae* (n = 3 individual colonies) from the North Pacific Subtropical Gyre. Amino acid names are in conventional three-letter abbreviation format. Essential and non-essential amino acids designated with ^{E} and ^{N}, respectively.

	PC1	PC2	PC3	PC4	PC5	PC6	PC7	PC8	PC9	PC10	PC11
Ala^{N}	0.19	-0.45	0.35	-0.63	0.45	0.06	-0.09	-0.07	-0.15	-0.03	-0.10
Asp^{N}	-0.28	-0.36	-0.36	-0.02	0.19	0.31	0.04	0.65	0.20	-0.15	0.20
Glu^{N}	-0.12	-0.51	-0.60	0.04	-0.01	-0.23	-0.16	-0.51	0.03	0.11	-0.08
Gly^{N}	0.30	-0.32	0.15	0.39	0.20	-0.11	0.72	-0.05	0.23	0.04	-0.08
Ile^{E}	-0.37	0.02	-0.09	-0.13	-0.04	-0.14	0.37	0.22	-0.55	0.52	-0.25
Leu^{E}	-0.36	-0.06	0.29	-0.09	-0.14	0.41	0.00	-0.23	0.52	0.52	-0.01
Phe^{E}	-0.37	0.04	0.05	-0.06	-0.05	0.00	0.10	-0.04	0.17	-0.51	-0.74
Pro^{N}	-0.34	-0.10	0.32	0.59	0.49	-0.04	-0.38	-0.02	-0.20	0.04	-0.02
Ser^{M}	0.11	-0.53	0.31	0.19	-0.67	0.09	-0.17	0.17	-0.23	-0.06	-0.07
Thr^{E}	-0.37	-0.03	0.08	-0.04	-0.06	0.29	0.36	-0.40	-0.33	-0.39	0.46
Val^{E}	-0.35	-0.09	0.26	-0.18	-0.11	-0.75	0.03	0.13	0.27	-0.08	0.32
Variance	64.8%	25.5%	3.5%	2.2%	1.4%	1.1%	0.6%	0.5%	0.2%	0.1%	0.1%

279 Table C.6. Normalized essential amino acid $\delta^{13}C$ values of source end-members. Normalized $\delta^{13}C$ values of source end-members
280 (mean of five essential amino acid $\delta^{13}C$ values subtracted from individual essential amino acid $\delta^{13}C$ values for each sample) used as
281 the molecular-isotopic training data set in the mixing model of relative contribution of primary producers to deep sea corals
282 (superscript reference: a) Larsen et al. 2009; b) Lehman 2009, c) Larsen et al. 2013). The three source end-members (cyanobacteria,
283 eukaryotic microalgae, and heterotrophic bacteria) were analyzed in triplicate (mean ‰ ± SD).

Group	Latin name	Phylogeny	threonine	isoleucine	valine	phenylalanine	leucine
Cyanobacteria[c]	*Anabaena cylindrica*	Cyanobacterium	12.7 ± 1.0	1.3 ± 0.1	-1.9 ± 0.2	-7.4 ± 0.1	-4.7 ± 0.3
Cyanobacteria[c]	*Nostoc muscorum*	Cyanobacterium	11.5 ± 0.1	1.6 ± 0.1	-2.6 ± 0.1	-6.4 ± 0.2	-4.2 ± 0.0
Cyanobacteria[b]	*Cyanothece sp*	Cyanobacterium	11.0 ± 0.2	3.7 ± 0.1	-2.6 ± 0.2	-59 ± 0.3	-6.4 ± 0.2
Cyanobacteria[b]	*Trichodesmium sp.*	Cyanobacterium	11.9 ± 0.1	2.1 ± 0.2	-2.4 ± 0.2	-6.4 ± 0.2	.-5.0 ± 0.1
Cyanobacteria[b]	*Prochlorococcus sp.*	Cyanobacterium	17.3 ± 0.3	-0.3 ± 0.1	-2.8 ± 0.1	-7.2 ± 0.1	-6.9 ± 0.2
Cyanobacteria[b]	*Synechococcus sp.*	Cyanobacterium	16.5 ± 0.2	0.7 ± 0.1	-1.4 ± 0.2	-8.9 ± 0.2	-6.8 ± 0.1
Cyanobacteria[c]	*Merismopedia punctata*	Cyanobacterium	17.9 ± 0.6	-1.5 ± 0.0	-1.4 ± 0.1	-6.5 ± 0.1	-8.6 ± 0.0
Euk microalgae[c]	*Dunaliella sp.*	Chlorophyte	9.8 ± 0.5	0.7 ± 1.3	-2.7 ± 0.5	-0.4 ± 0.1	-7.2 ± 0.3
Euk microalgae[c]	*Prasinocladus marinus*	Chlorophyte	13.2 ± 0.8	0.1 ± 0.5	-5.2 ± 0.1	-0.1 ± 0.0	-7.9 ± 0.1
Euk microalgae[c]	*Melosira varians*	Diatom	9.1 ± 0.9	-0.4 ± 0.1	-3.6 ± 0.2	1.1 ± 0.2	-6.0 ± 0.0
Euk microalgae[c]	*Emiliana huxleyi*	Haptophyte	10.4 ± 0.1	1.2 ± 0.6	-5.4 ± 0.0	1.6 ± 0.0	-7.7 ± 0.0
Euk microalgae[c]	*Isochrysis galbana*	Haptophyte	12.2 ± 0.2	2.8 ± 0.1	-5.7 ± 0.1	1.2 ± 0.0	-10.3 ± 0.1
Het bacteria[a]	*Rhodococcus spp.*	Actinobacteria	5.3 ± 0.1	-1.2 ± 0.1	-0.7 ± 0.2	-3.1 ± 0.1	-0.1 ± 0.2
Het bacteria[a]	*Actinobacteria*	Actinobacteria	5.9 ± 0.4	-1.5 ± 0.2	-1.3 ± 0.1	-3.0 ± 0.1	0.0 ± 0.2
Het bacteria[a]	*Burkholderia xenovorans*	Betaprotobacteria	4.6 ± 0.8	0.2 ± 0.2	-1.6 ± 0.1	-4.6 ± 0.0	1.5 ± 0.1
Het bacteria[a]	*Escherichia coli*	Gammaproteobacteria	1.8 ± 0.5	1.0 ± 0.3	-0.1 ± 0.2	-2.0 ± 0.3	-0.5 ± 0.2

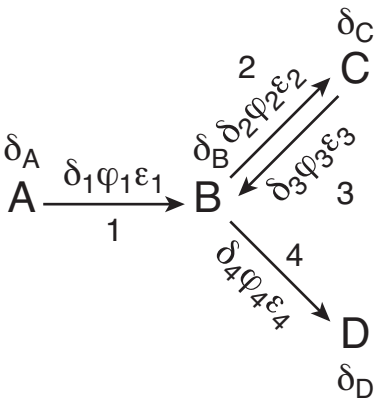

Figure C.1. A general schematic of a network of reactions leading to deep-sea coral polyp tissue and proteinaceous skeleton synthesis (after Hayes 2001). Node A represents the external dietary amino acid pool, node B represents the internal central amino acid pool from which tissues are synthesized, node C represents the metabolically active coral polyp tissue, and node D represents the proteinaceous skeleton. Isotopic compositions of these pools are indicated by δ (‰) with corresponding letter subscripts. Kinetic isotope reactions are designated by numbers with the δ, ϕ, and ε symbols with numerical subscripts indicating the isotopic compositions of the nitrogen being transmitted by a reaction, the flux of nitrogen being transmitted (moles/time), and the isotope effect (‰) associated with the reaction, respectively. The flux of AAs between the central AA pool and polyp tissues is represented as a bidirectional process for this metabolically active tissue. Conversely, the flux of AAs from the central AA pool into accretionary skeleton is represented as a unidirectional process, as the proteinaceous skeleton is metabolically inert post-deposition. Both the polyp and skeleton protein are likely synthesized from a shared central AA pool, which contains a mix of dietary AAs and AAs remobilized from reworked polyp tissue that has already undergone trophic enrichment. As a result, the higher flux of AA N into polyp tissue may mean that polyp tissue is getting a higher flux of trophic-enriched AAs through this bidirectional linkage with the central AA pool than skeleton material.